



UNIVERSIDADE ESTADUAL PAULISTA
"JÚLIO DE MESQUITA FILHO"
Câmpus de São José do Rio Preto

Alice Barra Freire

***Rhynchosaurus articeps* (Archosauromorpha, Rhynchosauria)
reanalyzed by computed tomography: Anatomy and Phylogeny**

São José do Rio Preto
2023

Alice Barra Freire

***Rhynchosaurus articeps* (Archosauromorpha, Rhynchosauria)
reanalyzed by computed tomography: Anatomy and Phylogeny**

Dissertação apresentada como parte dos requisitos para obtenção do título de Mestre em Nome do Programa de Pós-Graduação em Biodiversidade, do Instituto de Biociências, Letras e Ciências Exatas da Universidade Estadual Paulista “Júlio de Mesquita Filho”, Câmpus de São José do Rio Preto.

Financiadora: CAPES/PROEX

Orientador: Prof. Dr. Felipe Chinaglia Montefeltro

São José do Rio Preto
2023

Freire, Alice.

Rhynchosaurus articeps (Archosauomorpha, Rhynchosauria)
reanalyzed by computed tomography: Anatomy and Phylogeny/
Alice Freire. -- São José do Rio Preto, 2023
65 p.

Dissertação (mestrado) - Universidade Estadual Paulista
(Unesp),
Instituto de Biociências, Letras e Ciências Exatas, São José do
Rio Preto

Orientador: Felipe Montefeltro

1. Rhynchosaurial. I. *Rhynchosaurus articeps*
(Archosauomorpha, Rhynchosauria) reanalyzed by computed
tomography: Anatomy and Phylogeny

Alice Barra Freire

***Rhynchosaurus articeps* (Archosauromorpha, Rhynchosauria)
reanalyzed by computed tomography: Anatomy and Phylogeny**

Dissertação apresentada como parte dos requisitos para obtenção do título de Mestre em Nome do Programa de Pós-Graduação de Biodiversidade, do Instituto de Biociências, Letras e Ciências Exatas da Universidade Estadual Paulista “Júlio de Mesquita Filho”, Câmpus de São José do Rio Preto.

Financiadora: CAPES/PROEX

Comissão Examinadora

Prof. Dr. Felipe Chinaglia Montefeltro
UNESP – Câmpus de Ilha Solteira
Orientador

Prof. Dr. Júlio Cesar de Almeida Marsola
UTFPR – Câmpus Dois Vizinhos

Dr. Giovanne Mendes Cidade
UNESP – Câmpus de Ilha Solteira

São José do Rio Preto
4 de maio de 2023

AGRADECIMENTOS

Aos meus familiares, especialmente minha mãe, que sempre acreditou em meu esforço e me deu força nas dificuldades que tive durante o trabalho.

As minhas amigas e colegas da República XX, em especial Aline Parra por me acolher. Aos meus paleoamigo do Laborario de Paleontologia de Ilha Solteira Gabriel, Otavio, Juan, Kawan e Marcos. A minha amiga Beatriz.

Agradeço em especial ao meu orientador Felipe Montefeltro pela paciência e ajuda em momentos difíceis ao longo deste trabalho.

O presente trabalho foi realizado com apoio da Coordenação de Aperfeiçoamento de Pessoal de Nível Superior - Brasil (CAPES) - Código de Financiamento 001

“Nothing in Biology Makes Sense Except in the Light of Evolution”

Theodosius Dobzhansky

RESUMO

Rhynchosauria compõe um grupo de Archosauromorpha restrito aos depósitos triássicos, sendo que a origem e irradiação do grupo ocorreu no contexto das mudanças faunísticas drásticas causadas pela extinção em massa do Permo-Triássico. Rhynchosauria alcançou uma ampla distribuição geográfica no Triássico Superior, representando os consumidores primários mais abundantes em algumas partes do Pangeia. Este claro sucesso do grupo tem sido relacionado ao surgimento de um aparato mastigatório peculiar, formado por sulcos maxilares e cristas dentárias, sem paralelos em qualquer outro grupo de vertebrados. A monofilia de Rhynchosauria é bem estabelecida, com a presença também do clado Rhynchosauridae, que congrega todos os rincossauros com o aparato mastigatório peculiar. As variações morfológicas observadas no aparato mastigatório dos Rhynchosauridae são uma das principais fontes de caracteres filogeneticamente relevantes para o grupo. *Rhynchosaurus articeps* é o membro mais basal de Rhynchosauridae; entretanto, dos 16 espécimes conhecidos do táxon, apenas o lectótipo (SHYMS 1) representa um crânio completo, não deformado e com o aparato mastigatório completo. Porém, este espécime foi preservado com as mandíbulas adpressas; logo, não é possível reconhecer os estados de caracteres do aparato mastigatório peculiar presente na origem de Rhynchosauridae e formular explicações de como esta estrutura única do grupo surgiu. Este projeto investigou a anatomia do aparelho mastigatório do espécime de *Rhynchosaurus articeps* SHYMS 1 através de dados de microtomografia computadorizada, ampliando o conhecimento sobre a anatomia do táxon, evolução do aparelho mastigatório em Rhynchosauria com base em uma nova análise filogenética do grupo.

Palavras-chave: Rhynchosauridae. Anisiano. Archosauromorpha. Aparato mastigatorio.

ABSTRACT

Rhynchosauria is a group of Archosauromorpha, restricted to Triassic deposits. The origin and irradiation of the group occurred in the context of the drastic faunal changes caused by the Permo-Triassic mass extinction. Rhynchosauria reached a broad geographical distribution during the Upper Triassic, representing the most abundant primary consumers in parts of the Pangea. The ecological success of the group has been related to the emergence of a peculiar masticatory apparatus, formed by jaw blades and maxillary grooves. The monophyly of Rhynchosauria is well established, with the existence of the Rhynchosauridae clade nesting all rhynchosaurs with the peculiar masticatory apparatus. The morphological variation observed in the masticatory apparatus in Rhynchosauridae are one of the main sources of phylogenetically relevant characters for the group. *Rhynchosaurus articeps*, is the basalmost member of Rhynchosauridae, however among the 16 specimens known of this taxon, only the SHYMS 1, the lectotype, represents a complete skull, not deformed and with a complete masticatory apparatus preserved. However, this specimen was fossilized with the jaws in occlusion, so it is not possible to recognize the character states, of the peculiar masticatory apparatus, present at the base of Rhynchosauridae, and to formulate explanations of how this unique structure of the group emerged. This project investigated the anatomy of the masticatory apparatus of the specimen of *Rhynchosaurus articeps* SHYMS 1 through computed microtomography data, increasing knowledge about the anatomy of the taxon, evolution of the masticatory apparatus in Rhynchosauria based on an updated phylogenetic analysis.

Keywords: Rhynchosauridae. Anisian. Archosauromorpha. masticatory apparatus.

LIST OF ILLUSTRATIONS

Figure 1 – Phylogenetic and anatomical context of <i>Rhynchosaurus articeps</i>	15
Figure 2 – Map of England showing the area from which the remains of <i>Rhynchosaurus articeps</i>	18
Figure 3 – Skull of the Lectotype of <i>Rhynchosaurus articeps</i> SHYMS 1	18
Figure 4 – 3D rendering of the cranial elements of the Lectotype of <i>Rhynchosaurus articeps</i> SHYMS 1	19
Figure 5 – Flowchart of the scanning technique for the <i>Rhynchosaurus articeps</i> SHYMS 1 specimen.	21
Figure 6 – Skull of the Lectotype of <i>Rhynchosaurus articeps</i> SHYMS 1	28
Figure 7 – Lower jaw of the Lectotype of <i>Rhynchosaurus articeps</i> SHYMS 1	31
Figure – 8 Skull of the Lectotype of <i>Rhynchosaurus articeps</i> SHYMS 1	32
Figure 9 – Schematic drawings of the left maxillary dental plate	34
Figure 10 – Strict consensus of the 6 most parsimonious trees found in this analysis	36

SUMMARY

1	INTRODUCTION	13
2	GOALS	16
3	MATERIAL AND METHOD	17
3.1	Material	17
3.2	Method	20
3.2.1	Virtual preparation	20
3. 2. 2	Phylogeny	22
4	DESCRIPTION	25
4.1	Maxillary dentition	25
4.2	Pterygoid dentition	29
4.3	Dentary dentition	29
5	DISCUSSION	33
5.1	Masticatory apparatus evolution in basal Rhynchosauria	37
6	CONCLUSION	39
	REFERENCES	40
	ATTACHMENT A - Character list used in the parsimony analysis	44
	ATTACHMENT B - SYNAPOMORPHY LIST	53
	ATTACHMENC A - OTUs USED IN THE PHYLOGENETIC	59
	ANALYSIS	
	ATTACHMENT D - TAXON-CHARACTER MATRIX	60
	ATTACHMENT E - Most Parsimonious trees	64

1 INTRODUCTION

Rhynchosauria is a peculiar group of Archosauromorph diapsids temporally restricted to the Triassic period (Ezcurra et al., 2016; Butler et al., 2015). The fossil record of the group indicates an important diversity since the early Middle Triassic, with three South African forms found in Anisian deposits of the Burgersdorp Group (Dilkes 1995, Butler et al., 2015, Ezcurra et al., 2016). Still in the Middle Triassic, the group expands geographically and in diversity, with records known from Anisian deposits in England, the United States, Tanzania, Brazil and Argentina (Ezcurra et al., 2014, 2016, Schultz et al., 2016). However, the Hyperodapedontinae subgroup (*sensu* Langer et al., 2017), became particularly diverse in the Late Triassic (Carnian). During the Carnian, rhynchosaurs dominated the space of primary consumers in much of Pangea, with some deposits of this age in Brazil and Argentina, but records of the group are also recognized in the United States, Canada, Scotland, Tanzania, Zimbabwe, Madagascar, and India. (Lucas et al., 2002, Langer et al. 2000; Montefeltro et al. 2010; Langer et al., 2017; Sues et. al., 2020; Fitch et. al.; 2023). This apparent explosive irradiation of the group, since its origin, has been attributed to the context of drastic faunal changes caused by the Permo-Triassic mass extinction (Ezcurra et al., 2016, Ezcurra & Butler 2018).

The monophyly of the Rhynchosauria group is well established since the first phylogenetic works on the group (Dilkes 1998, Benton, 1990, Langer & Schultz 2000). Additionally, the interrelationships of their subgroups present a certain consensus among the most recent phylogenetic analyzes (Montefeltro et al., 2010, 2013; Butler et al., 2015; Schultz et al., 2016, Langer et al., 2017; Sues et. al., 2020; Fitch et. al., 2023). In these works, the three South African taxa are consistently recovered as successive sister groups of Rhynchosauridae, and the existence of a major dichotomy between two major clades in Rhynchosauridae: non-Stenaulorhynchinae Hyperodapedontidae and Stenaulorhynchinae (senso Montefeltro et al., 2010 and Schultz et al., 2016).

When the anatomy of the group is analyzed from a phylogenetic perspective, it is possible to recognize the transformation of a more generic Diapsida anatomy, recognized in non-Rhynchosauridae Rhynchosauria taxa, to the more derived, and anatomically specialized taxa of the Rhynchosauridae (Butler et al., 2015 , Schultz et al., 2016, Langer et al., 2017), which have maxillae with batteries of teeth and

longitudinal grooves, and dentaries with blades that fit into the maxillae (Benton 1984, Nesbit & Whatley 2004, Langer et al. 2000).

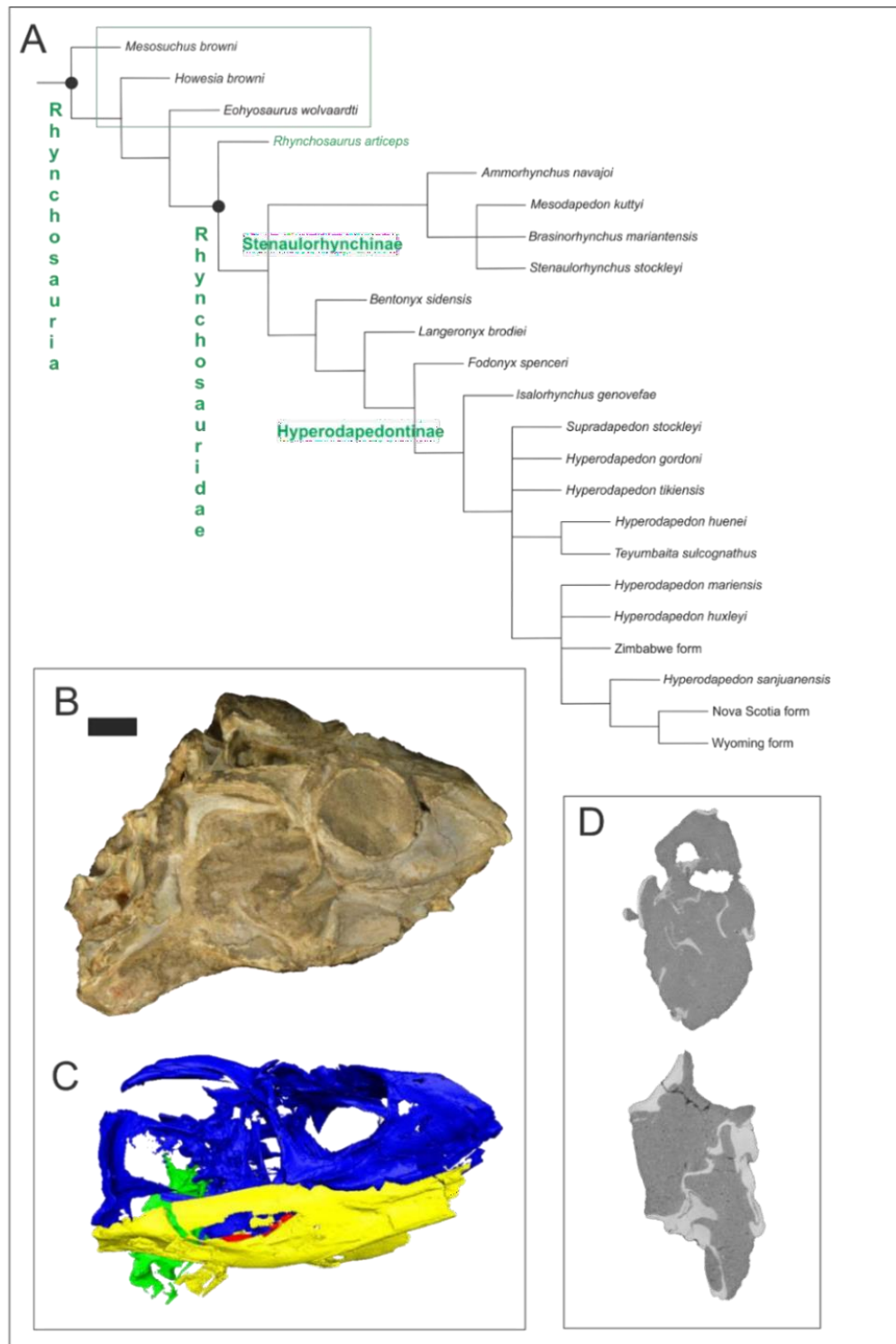
This type of masticatory apparatus found in Rhynchosauridae is unique and has no analogue among fossil or living amniotes (Benton 1984). In fact, the evolutionary success of the group throughout the Triassic has been related to the presence of this peculiar masticatory apparatus, which would have allowed rhynchosaurs to become the dominant primary consumers in much of Pangea (Dilkes 1998, Ezcurra et al., 2016, Schultz et al., 2016, Langer et al., 2017).

Additionally, due to the great diversity of the anatomy of the masticatory apparatus among the Rhynchosauridae, the phylogenetic relationships of the group are largely based on characters recognized in this anatomical region. For example, in one of the broader phylogenies of the group, of the 123 phylogenetically relevant characters identified, 43 are related to the masticatory system (Langer et al., 2017).

Rhynchosaurus articeps was the first rhynchosaurian taxon to be described (Owen, 1842) and its occurrences are restricted to the Tarporley Siltstone Formation (Anisian, 247-200 mya, Ezcurra et al., 2016), that crops out in central England. There are 16 specimens attributed to this taxon but only the lectotype SHYMS 1 (Shropshire Museums, Ludlow, England), represents a complete skull, relatively undeformed and with the masticatory apparatus completely preserved. However, the lectotype of the taxon was preserved with the occluded mandibles, so that most of the characters related to the taxon's masticatory apparatus are included in the phylogenetic analyzes as missing data.

Our goal is to describe the masticatory apparatus of the lectotype of *Rhynchosaurus articeps* SHYMS 1, via data acquired via Computed Tomography Scan (CT scan), with the aim to understand the anatomy of the masticatory apparatus at the origins of Rhynchosauridae. The CT scan data are particularly useful for recognizing the inaccessible anatomy of the lectotype, the most important specimen of *Rhynchosaurus articeps*, allowing access to the anatomy of the masticatory apparatus. With the new anatomical data, we developed an updated phylogenetic analysis of Rhynchosauridae to understand the impact of the new observations on the evolution of the masticatory apparatus of the group.

Figure 1 – Phylogenetic and anatomical context of *Rhynchosaurus articeps*. A: Phylogeny of Rhynchosauria modified from Langer et al. (2017). B: Right side view of the *R. articeps* SHYMS 1 lectotype. C: Right side view of the 3D reconstruction of the *R. articeps* SHYMS 1 lectotype; Scale bar 1cm. D: CT slices of the lectotype of *R. articeps* SHYMS 1.



Source: Own author.

2 GOALS

The objectives of this work are related to the tomography data obtained from the lectotype of *Rhynchosaurus articeps* and aim to:

- Virtual preparation of the SHYMS 1 specimen;
- Description of the taxon masticatory apparatus to recognize the number of longitudinal grooves in the maxilla; number of teeth, relative position and morphology of medial and lateral areas to(of?) the maxillary groove; presence or absence of maxillary lingual teeth; number of dentary blades, absence/presence of dentary lingual teeth.
- Recognition of the conditions present in *R. articeps* regarding the phylogenetically relevant characters of the masticatory apparatus, and incorporation of these data in one of the most recent phylogenetic matrices of the group (Langer et al., 2017). With this, we intend to develop an updated parsimony analysis of Rhynchosauria and the reassessment of the phylogenetic position of *R. articeps*;
- With the updated phylogenetic matrix and developed analysis, recognize the plesiomorphic conditions of the anatomy of the masticatory apparatus of Rhynchosauridae and recognize the evolution of these characters in Rhynchosauria.

3 MATERIAL AND METHOD

3.1 Material

The material analyzed is the lectotype of *Rhynchosaurus articeps* SHYMS 1 (Figure 1 B), recovered from Grinshill, North Shropshire (Figure 2), and deposited at the Shropshire Museums, Ludlow in England, from the Tarporley Siltstone Formation (Anisian, 247-200 mya, (Ezcurra et. al., 2016)).

This specimen is represented by a complete skull relatively well preserved and slightly deformed, but with the jaws attached to the skull. The description of the dental morphology of the lectotype *Rhynchosaurus articeps* SHYMS 1 is based on a three-dimensional model rendered from a Computed tomography (CT scan), the CT scan was used to digitally disarticulate the skull from the lower jaw and reconstruct most of the masticatory apparatus of the taxon (Figure 3 and 4).

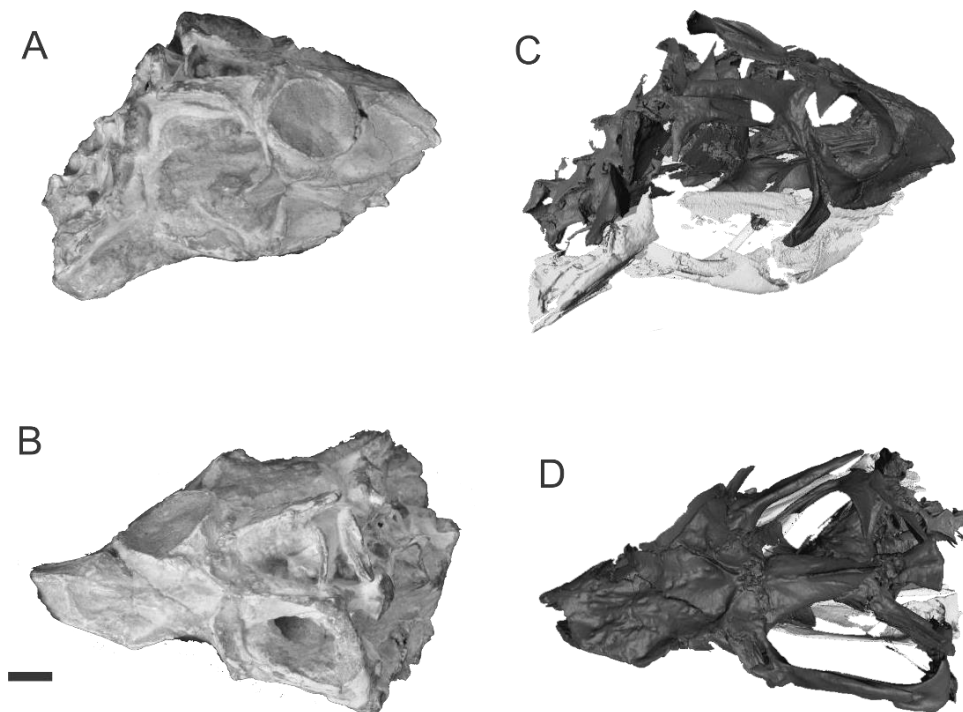
Computed tomography data of the lectotype *Rhynchosaurus articeps* (SHYMS 1), was performed at the University of Bristol in January 2019, in a micro tomograph of the Nikon XTH 225ST, in which a total of 3141 projections were obtained, and transformed into 1999 slices (slices) 0.05 mm thick (voltage of 224 kV and a current of 170 mA). The processing of CT scan data of the skeletal elements was carried out in Amira 5.3.3 for the generation of three-dimensional models, which segment the bone matrix, being able to isolate specific elements digitally (Figure 4, 6, 7 and 8).

Figure 2 – Map of England showing the area from which the remains of *Rhynchosaurus articeps* SHYMS 1, described in this work, were recovered: point in red Grinshill, north of Shropshire.



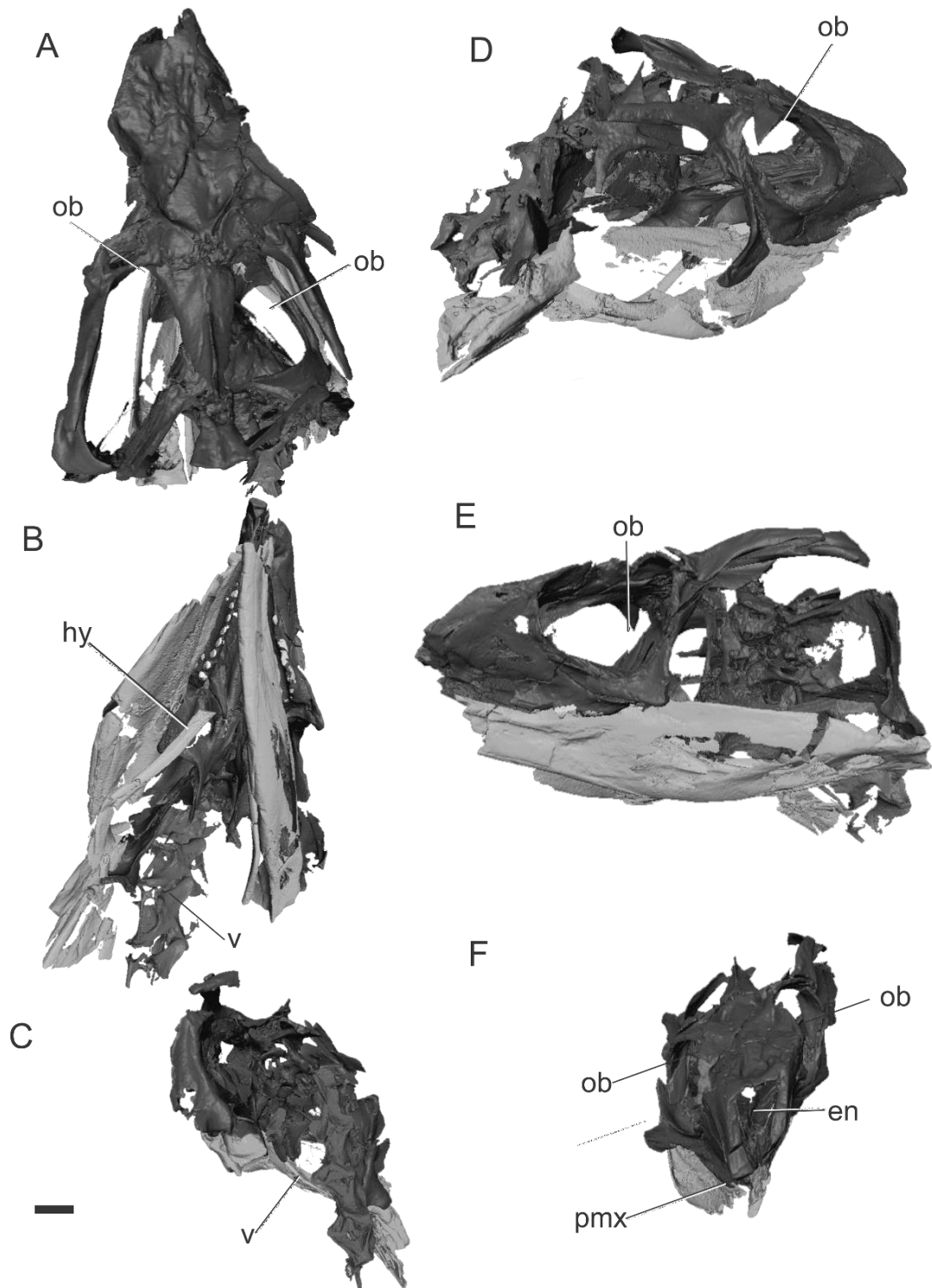
Source: Modified from Benton (1990).

Figure 3 – Lectotype of *Rhynchosaurus articeps* SHYMS 1: A: Right lateral view; B: Dorsal view. 3D rendering of the cranial elements of the Lectotype of *Rhynchosaurus articeps* SHYMS 1: C: Right lateral view; D: Dorsal view. Scale bar = 1 cm.



Source: Own author.

Figure 4 – 3D rendering of the cranial elements of the Lectotype of *Rhynchosaurus articeps* SHYMS 1: A: Dorsal view; B: Ventral view; C: Posterior view; D: Right lateral view; E: Left lateral view; F: anterior view. Abbreviations: en, external naris; hy, hyoid; ob, orbit; pmx, premaxilla; v, vertebra. Scale bar = 1 cm.



Source: Own author.

3.2 Methods

3.2.1 Virtual Preparation

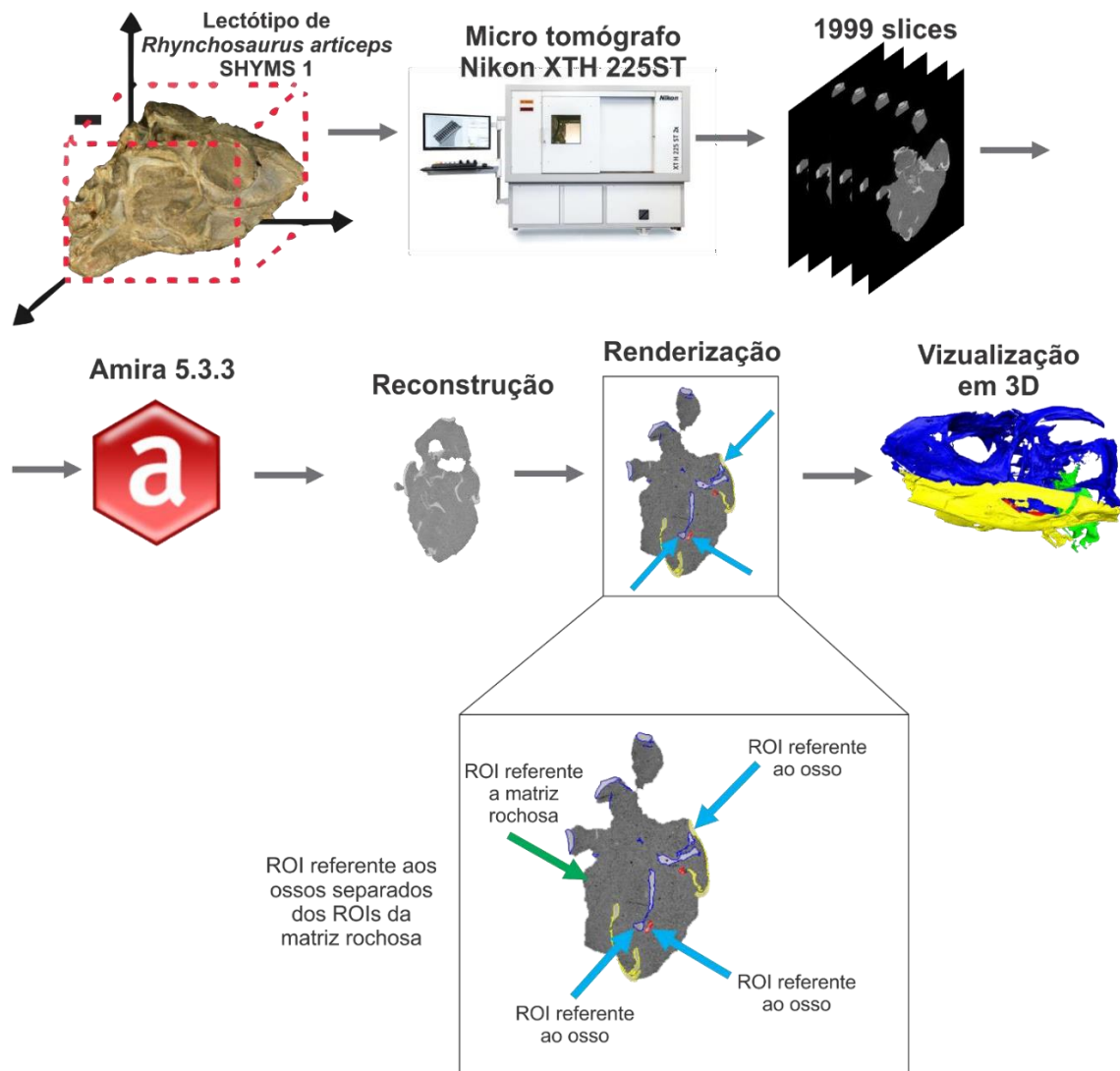
The restoration of fossils with digital techniques is gradually gaining space to answer taxonomic, systematic and evolutionary questions. However, the criteria used for restorations, the protocols used and even the observed restrictions are usually not clear (Lautenschlager, 2016; Sutton, 2008; Sutton et al., 2016; Cunningham et al., 2014).

Computed tomography (CT scan) has been the most commonly applied technique to digitize fossil specimens in the last decade (Cunningham et al., 2014, Lautenschlager, 2016, Sutton, 2008; Sutton et al., 2016). This technique can be used as a preparation method that facilitates the non-destructive extraction of fossil specimens in rock matrix (Lautenschlager, 2016; Lautenschlager, 2017). Tomography is the digital representation of a three-dimensional structure, through numerous two-dimensional images formed from parallel sections (Lautenschlager, 2016; Sutton, 2008).

To study the anatomy of a fossil based on tomography, the preparation of a tomographic dataset is required (Sutton, 2008). The digital preparation consists of two phases: reconstruction and rendering. In the reconstruction, from computed tomography, regions of interest (ROI) are obtained. In the present project, the ROI corresponds to the bones of the fossil. This process aims to divide the voxels (equivalent to the pixel in 3D) present in the ROI based on the interest of the project, that is, to separate the voxels related to the bones, from the voxels related to the rock. To achieve this separation, the voxels are identified by common properties, based on the gray value of each voxel and/or position of the voxel within the slices (Sales & Schultz, 2014). With preparation it is possible to eliminate the rocky matrix. This ROI interpretation process, with the separation of voxels of interest, is called segmentation (Sutton, 2008).

Sequentially, in rendering, each voxel selected from the ROIs in the preparation phase are assigned to one or more surfaces. In the case of the present work, bony areas are identified in the skull as assigned to a surface. Thus, at the end of the preparation and rendering process, skull and lower jaw is reconstructed separately and can be viewed independently (Sutton, 2008; Lorensen & Cline, 1987) (Figure 5).

Figure 5 – Flowchart of the scanning technique for the *Rhynchosaurus articeps* SHYMS 1



Source: Own author.

3.2.2 Phylogeny

The starting point of the parsimony analysis is the matrix from Langer et al. (2017) that was updated in the present work. The new updated matrix was assembled in Mesquite 3.61 and subjected to parsimony analysis in TNT 1.5 software (Goloboff and Catalano, 2016). The search algorithm for the most parsimonious trees used was the Traditional Search using 1000 replicates with a random seed of 0 and a hold of 20. See Appendices for complete information on character list, operational taxonomic unities, and matrix.

The recognized and reconstructed anatomical features of *Rhynchosaurus articeps* SHYMS 1, and which proved to be phylogenetically relevant, were incorporated into the database and a parsimony analysis was developed to reassess the taxon scorings. For this phylogenetic analysis, the final matrix includes 25 taxa and 129 characters; among the taxa, *Protorosaurus speneri* and *Prolacerta broomi* are non-rhincosaurian outgroups.

Additionally, six new characters have been added to the dataset:

- **124:** Maxilla, posterior half of the lateral tooth bearing area: entire transverse surface covered with teeth (0); presence of an edentulous lateral platform (1)
- **125:** Jugal, anterolateral surface of the posterior process: mostly flat (0); with a posterodorsally well rimmed depression that merges gradually anteriorly with the main body of the bone (1)
- **126:** Quadratojugal, shape of the main body: subtriangular, with a broad dorsal ramus (0); crescent-shaped, with a strongly anteriorly curved and anteroposteriorly narrow dorsal ramus (1).
- **127:** Parabasisphenoid, position and orientation of the entrance of the internal carotid arteries: on the ventral surface and immediately posteromedial to the bases of the basipterygoid processes, facing mainly ventrally (0); on the ventral surface and between the bases of the basipterygoid processes close to the level of their mid-length, facing mainly anteriorly (1)
- **128:** Parabasisphenoid, distal end of the basipterygoid processes in ventral view: well-separated from each other, clearly exposing the ventral surface of the parabasisphenoid between them (0); almost touching each other in the median line and restricting the interbasipterygoid process space to a narrow furrow, also

resulting in basal articulation of the pterygoids approaching very close to each other (1)

- **129:** Scapula, lateral development of the acromion process: low and not more developed than the transverse thickness of the scapular neck (0); hypertrophied as a shelf-like structure more developed than the thickness of the scapular neck (1)

For phylogenetic reanalysis, scoring of *Langeronyx brodiei* was also changed to the following states, based on new photographs of the holotype NHM 8495 and of the specimen R2623: character 14 (? -> 0), 108 (? -> 0), 112 (? -> 1), 113 (? -> 0), 115 (? -> 0) and 124 (? -> 0). In addition, the character scoring of *Bentonyx sidensis* was also reevaluated and the following characters changed, based on the CT-Scan of the holotype BRSUG 27200: 65 (?-> 1), 66 (?-> 1), 67 (?-> 0), 69 (?-> 0), 70 (1-> 2), 73 (?-> 0), 74 (?-> 0), 75 (?-> 0), 76 (?-> 2), 78 (?-> 1) and 80 (0-> 1) .

The reevaluation of the *Rhynchosaurus articeps* based on the CT scan allowed a more precise scoring of the traits assigned to the taxon in our analysis. As such, we rescored the following characters:

- 45 (?-> 1): Pterygoid midline suture length less than the distance between the caudal margin of the suture and the basipterygoid articulation
- 64 (?-> 0): Pterygoid teeth present as two rows of bottom-like teeth
- 65 (?-> 0): Medial maxillary groove absent
- 66 (?-> not applicable).
- 67 (?-> 0): Maxillary area lateral to main groove narrower than the medial area
- 71 (?-> 1): Occlusal tooth rows on the rostral half of the maxilla, fewer than four tooth rows
- 72 (?-> 1): Maxillary lingual teeth present
- 73 (?-> 1): Maxillary lingual teeth large number of teeth on the medial surface of the bone
- 74 (?-> 0): Maxillary teeth only conicals
- 75 (?-> 0): Dentary teeth: only conical
- 78 (?-> 1): Lingual dentary teeth present
- 79 (?-> 1): Lingual dentary teeth forming more than one row
- 80 (?-> 0): Dentary teeth on the dentary lingual surface forming rows of well-spaced teeth

- 83 (?-> 0): Cervical postaxial vertebrae ventral keel absent
- 108 (?-> 0): Extension of the maxillary groove along the whole occlusal surface of maxilla
- 109 (? -> 0): Maxillary cross-section medial to main groove crest-shaped
- 112 (?-> 0): Maxillary lingual tooth crown orientation, medially oriented, perpendicular to maxillary medial wall
- 115 (?-> 0): Proportion of maxillary tooth plate, width at caudal end divided by length, less than 0.3
- 121 (?-> 0): Number of tooth rows lateral to the main groove lesser than the number of medial tooth row
- 122 (?-> not applicable)
- 123 (?-> 1): Medial most row of occlusal tooth at caudal region of maxilla, medially displaced and crowns with not strictly occlusal direction
- 124 (? -> 0): Maxilla, posterior half of the lateral tooth bearing area, entire transverse surface covered with teeth (new character).
- 125 (?-> 0): Jugal, anterolateral surface of the posterior process mostly flat (new character).
- 126 (?-> 0): Quadratojugal, shape of the main body subtriangular, with a broad dorsal ramus (new character).
- 127 (?-> 0): Parabasisphenoid, position and orientation of the entrance of the internal carotid arteries, on the ventral surface and immediately posteromedial to the bases of the basiptyergoid processes, facing mainly ventrally (new character).
- 128 (?-> 0): Parabasisphenoid, distal end of the basiptyergoid processes in ventral view, well-separated from each other, clearly exposing the ventral surface of the parabasisphenoid between them (new character).

4 DESCRIPTION

The following description was based in the more complete left maxilla, in which is easier to differentiate the densities between the bone and the teeth by the shade of gray through the tomography. However, in order to obtain complete information, the right maxilla was also analyzed. In the dentary, the cutting blade and the lingual teeth are only preserved on the right element. Only the cutting blade is preserved on the left dentary so that fine anatomy of this structure is not always visible, such as the cushion-shaped medial wall of the dentary. However, given that the CT-Scan allow the visualization of the internal anatomy of the elements, the lingual teeth on the left dentary were reconstructed based on its roots within the bone.

Rhynchosaurus articeps, has the typical morphology of Rhynchosauridae with a beak-shaped edentulous premaxilla and skull longer than wide, and is the first Rhynchosauria described with a main groove in the maxilla, which dental blades fit perfectly in the main groove (Figure 1: B, C; 3 and 4). We observed the presence of teeth on the occlusal and lingual areas of the maxillae and dentaries, as well as on the ventral surface of the pterygoids, which will be described in detail in the following items.

The description of the distribution of the teeth follows Chatterjee (1974), in which the teeth are designated by the pattern of longitudinal rows lateral and medial to the main groove. For example, L1 refers to the first lateral row to the main groove, L2 the second row and so on sequentially; the same way occurs in the medial rows to the main groove called M1, M2, etc.

4.1 Maxillary dentition

The occlusal surface of the right maxillary dental plate has a length of 4,15 cm and a maximum transverse width at the posterior end of 0,9 cm; in the left maxilla the occlusal surface of the upper dental plate is 3,95 cm and 0,7 cm in maximum transverse width at the left posterior end. However, the total length of both maxillae in life were larger given that the anterior ends of both structures are damaged.

The maxilla is divided by a single deep, longitudinal main groove, which runs through the total length of the maxilla, curves laterally posteriorly, and gradually becomes shallower and narrower anteriorly. The groove separates the tooth bearing

areas of the maxillae (sensu Montefeltro et al., 2010), which differs from other Rhynchosauridae, as in some Hyperodapedontinae, *Hyperodapedon huenei*, *Hyperodapedon mariensis* (Langer et al., 2017), *Bentonyx sidensis* (Sethapanichsakul et al., 2023), *Fodonyx spenceri* (Langer, 2010) and *Teyumbaita sulcognathus* (Montefeltro et al., 2010) and the Stenaulorhynchinae, *Brasinorhynchus mariantensis* (Schultz et al., 2016) and *Stenaulorhynchus stockleyi* (Benton, 1984), which have two longitudinal grooves delimiting three areas of tooth bearing areas (Gentil & Ezcurra, 2017; Langer et al., 2017; Langer et al., 2000).

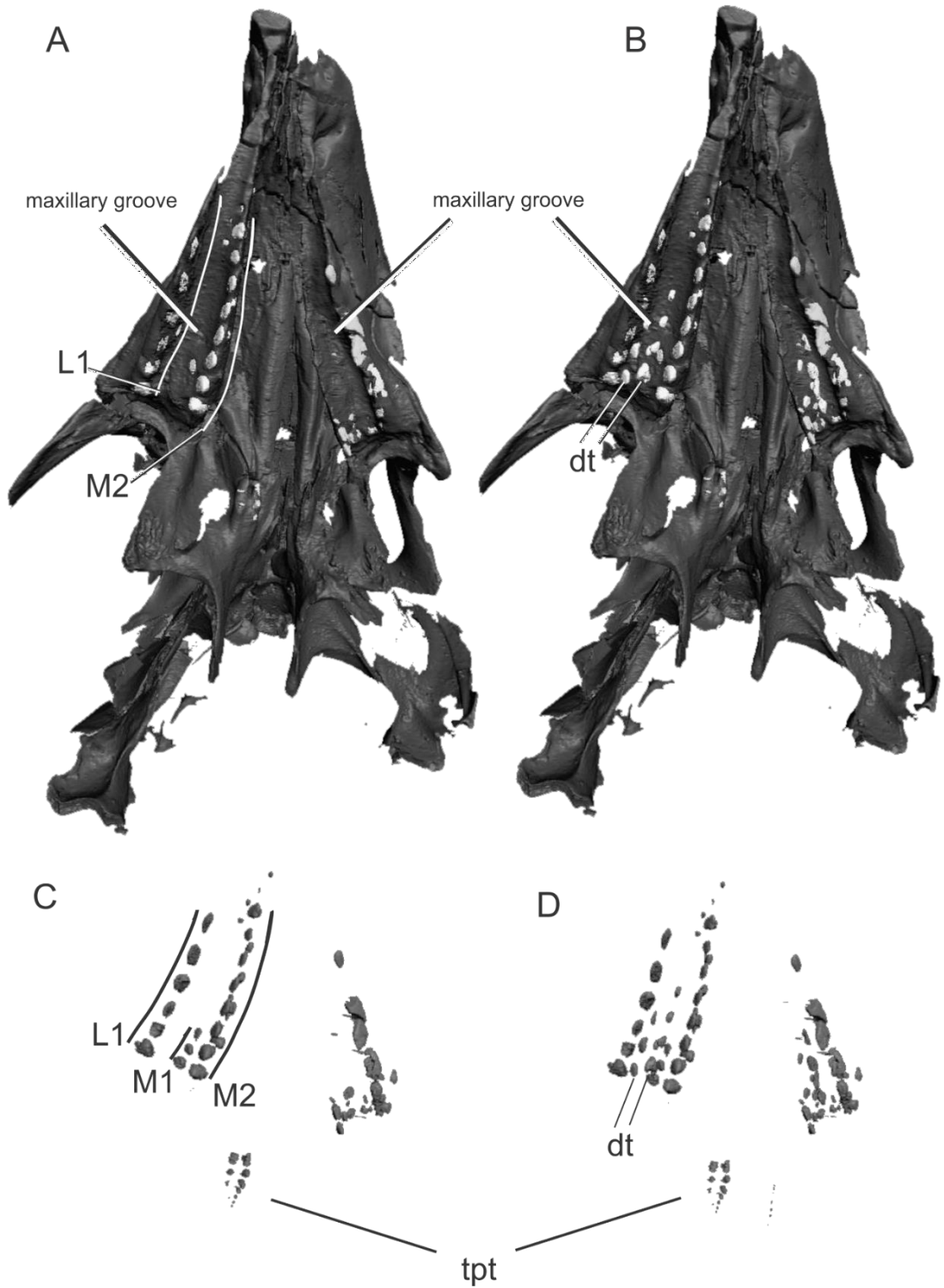
The lateral limit of the maxillary groove is more squared posteriorly and becomes gradually smoother anteriorly. Such changes in anatomy indicates greater wear in the anterior region during life (Benton, 1984; Montefeltro et al. 2010).

All observed teeth in *Rhynchosaurus articeps* SHYMS 1 are roughly conical in cross section, and no pyramidal tooth (sensu Scartezini and Soares, 2023) are present, differently from non-Stenaulorhynchinae Hyperodapedontidae (Whatley, 2005, Montefeltro et al., 2010, Langer et al., 2010, Scartezini and Soares, 2023). We identified a single lateral row of teeth (L1) in *Rhynchosaurus articeps* SHYMS 1. The L1 is formed by teeth of similar size and regularly spaced along the crest formed by the lateral maxillary tooth bearing area. However, the crowns of the teeth in L1 form the lateral wall of the maxillary groove. The medial tooth bearing area in *Rhynchosaurus articeps* SHYMS 1 presents three medial rows (M1-M3). The M1 is formed by teeth that are completely enclosed within the area of the longitudinal maxillary sulcus. Given the wear present in the longitudinal sulcus, the better observation of the teeth in M1 is possible by the roots of the teeth, as such only few crowns of the teeth in this row are observed in the outer surface of the rendered maxilla (Figure 6 and 8). The teeth of M2 present a similar pattern of the observed in L1, in which the tooth crowns limit the medial wall of the longitudinal groove. M3 is composed of lingual teeth on the lingual wall of the medial maxillary tooth bearing area.

Given the observed occlusion of the lower jaw in the maxillary groove (Figure 6 B and D), it is possible to infer that most of the maxillary groove area occluded with the dentary blade during mastication. However, the more posteriorly located maxillary teeth of the L1 and M1 and M2 are larger, with more complete crowns, showing less degree of wear (Benton, 1984; Montefeltro et al. 2010). This is due to the typical ankylotodont dentition of Rhynchosauria, in which the new teeth do not replace the

older teeth from below, but rather are added at the back of the rows of teeth. Therefore, the posterior-most teeth are the younger ones and did not suffer as much wear as more anterior located teeth in the maxillae tooth bearing areas (Benton, 1990). This is particularly evident in the anterior most region of both maxillae in which the tooth crowns are completely worn-off and only parts of the tooth roots are present. On the other side, all the teeth in M3 remained outside the occlusion area of the lower jaw blade, and the crowns do not show any sign of wear (Figure 8 A). This is a similar pattern to the one observed in other rhynchosaurs with lingual teeth on the maxillae, such as *Stenaulorhynchus stockleyi*, *Brasinorhynchus mariantensis*, *Ammorhynchus navajoi*, *Bentonyx sidensis*, *Langeronyx brodiei*, *Teyumbaita sulgonathus*, and *Hyperodapedon huenei* (Langer and Schultz, 2000, Montefeltro et al., 2010, Langer et al., 2010, Ezcurra et al., 2016, Schultz et al., 2016).

Figure 6 – Skull of the Lectotype of *Rhynchosaurus articeps* SHYMS 1: A: Ventral view of the skull with the maxillary and pterygoid teeth; B: ventral view of the skull with the maxillary, dentary and pterygoid teeth; C: Ventral view with maxillary teeth and pterygoids; D: Ventral view with the maxillary, dentary and pterygoid teeth; E: Left anterior view; F: lateral view. Abbreviations: dt, dental teeth; tpt, pterygoid teeth



Source: Own author.

4.3 Pterygoid Teeth

The pterygoid occupies a large area of the ventral surface of the skull. Each of the pterygoid bone has a antero-posteriorly directed projection, in the anterior region of this projection, the bones contact its counterpart. However, in the medial and posterior region of the skull, the pterygoids gradually diverge into two lateral projections forming the interpterygoid space between them. The posterior-most surface of the pterygoids form a ridged ventral surface.

The pterygoid teeth are present in the ridged ventral surface of the bone at its posterior region. However, the teeth seem to be externally visible only on the right pterygoid, while on the left side the pterygoid teeth do not seem to be erupted and can only be assessed via the CT-scan slides. On the right side, it is possible to see clearly two rows of rounded tooth crowns (Figure 6 C, D; 7 B and 8 A). The teeth are larger anteriorly and gradually decrease, until the smallest teeth in the posterior part. In the left pterygoid, it is only possible to observe a row of teeth with very small teeth along the entire series.

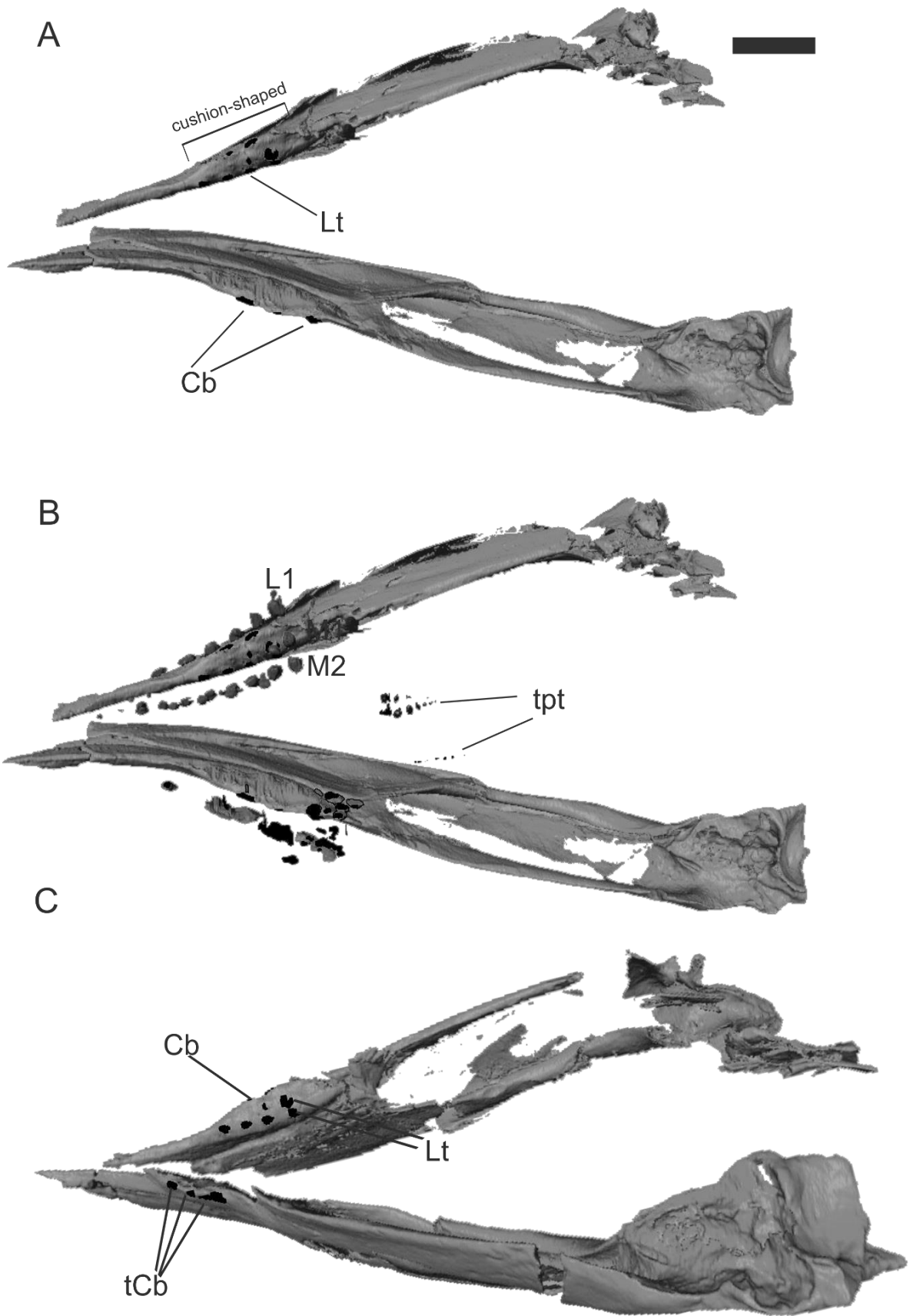
4.2 Dentary Dentition

The lectotype of *Rhynchosaurus articeps* possesses the typical characters of non-Hyperodapedontinae rhynchosaurs, such as its depth less than 0.25% in relation to its total length. The mandible, in lateral view, has a crescent shape curving dorsally at both ends (Benton, 1990), and the mandibular symphysis is formed mostly by the splenial, resulting in a divergence of the dentary in front of the symphysis. These two characters are also typical of Rhynchosauridae and present in *Rhynchosaurus articeps* (Benton, 1990; Langer et. al.; 2017). In non-Rhynchosauridae rhynchosaurs such as *Mesosuchus browni*, the mandibular symphysis is formed largely by the dentary, and there is no anterior divergence of the dentary anterior to the symphysis (Dilkes, 1998). There is no available data related to the divergence of the dentary in the other two basal non-Rhynchosauridae Rhynchosauria *Howesia browni* and *Eohyosaurus wolvaardtti*. The dentary of *Rhynchosaurus articeps*, in lateral view, has a total length of almost two thirds of the total length of the mandible, as in *Fodonyx spenceri* and hyperodapedontine taxa, however this proportion is different in the Stenaulorhynchinae *Stenaulorhynchus*, in which the dentary occupies half of the mandible (Benton 1990).

The dentary teeth are observed in two distinct regions of the bone. There is a single row of dentary teeth longitudinally distributed on top of the single dentary cutting blade (Figure 7), and two longitudinal tooth rows of lingual teeth on the cushion-shaped medial wall of the dentary (sensu Langer and Schultz, 2000, Montefeltro et al., 2010). However, given the typical ankylotherapsid dentition also present in the dentary, tooth crowns are only visible in the posterior half of the dentary, while anteriorly, the tooth crowns were completely worn-off (Figure 5: D and E; Figure 6: D and B Figure 7). All dentary teeth are conical in shape, with a slightly longer rostrocaudal main axis. There is no differentiation between pencilate (sensu Scartezini and Soares 2023) and conical teeth in the dentary. This condition is different from what is observed in most hyperodapedontidae rhynchosaurs (Whatley, 2005, Scartezini and Soares 2023). The spacing between teeth in the same row is smaller among teeth on the cutting blade, while lingual teeth are slightly closer to each other (Figure 7).

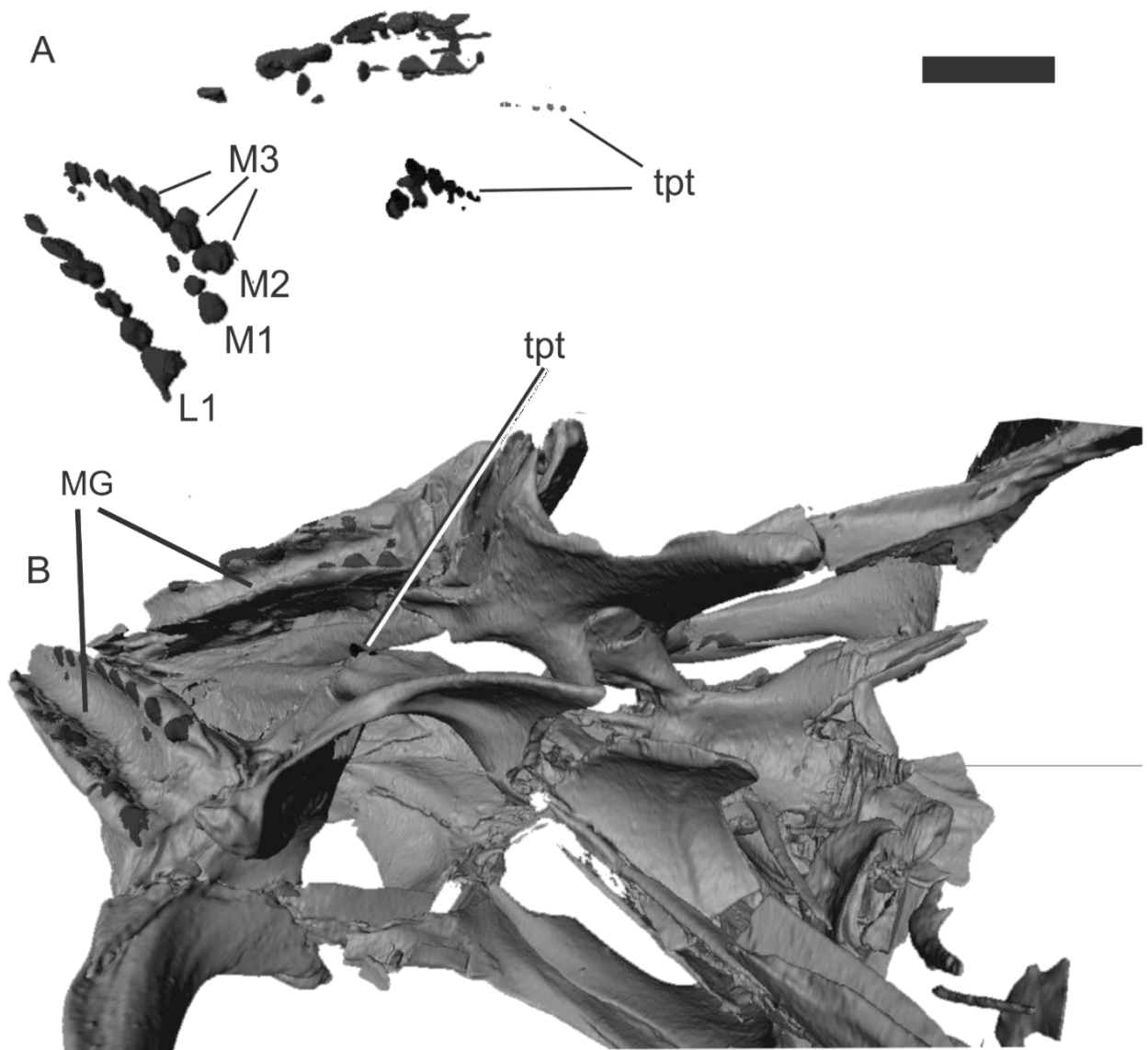
In dorsolateral view, the right dentary is cushion-shaped; however, that trait is more developed on its posterior half, while anteriorly the cushion-shaped surface gradually merges with the dorsal surface of the dentary. The presence of the cushion-shaped morphology in *Rhynchosaurus articeps* was for the first time observed, and rescored from Langer et. al. (2017), in which the dentary was described as having a flat shape in its caudal portion (Benton 1990; Langer et. al. 2017). This characteristic of the dentary is similar only to few species among Rhynchosauria, such as *Fodonyx spenceri*, and in the stenaulorhynchines, *Stenaulorhynchus stockleyi* and *Brasinorhynchus mariantensis*, and in the hyperodapedontine *Teyumbaita sulcognathus* (Langer et. al.; 2017), while all other rhynchosaurs possess a flat lingual surface along the entire length. Given the articulation of the skull and lower jaw in the lectotype of *Rhynchosaurus articeps*, it is possible to observe that all tooth rows, both on the cutting blade and on the lingual teeth, occlude on the main maxillary groove.

Figure 7 – Lower jaw of the Lectotype of *Rhynchosaurus articeps* SHYMS 1: A: Dorsal view lower jaw; B: Dorsal view lower jaw with the maxillary and pterygoid teeth; C: Lingual view lower jaw Abbreviations: Lt, lingual teeth; tpt, pterygoid teeth; Cb, cutting blade; tCb, cutting blade teeth. Scale bar = 1 cm.



Source: Own author.

Figure – 8 Skull of the Lectotype of *Rhynchosaurus articeps* SHYMS 1: A: Ventral view of the maxilar and pterygoid teeth; B: Ventral view of the skull with the maxilar and pterygoid teeth; Abbreviations: dt, dental teeth; tpt, pterygoid teeth; MG, maxillary groove. Scale bar = 1 cm.



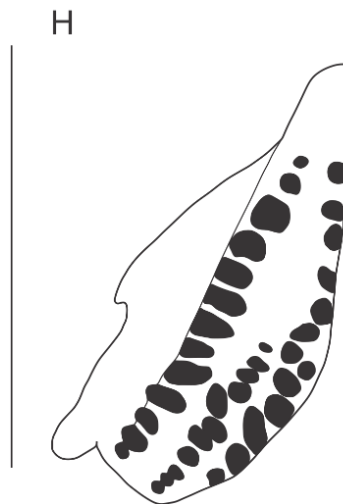
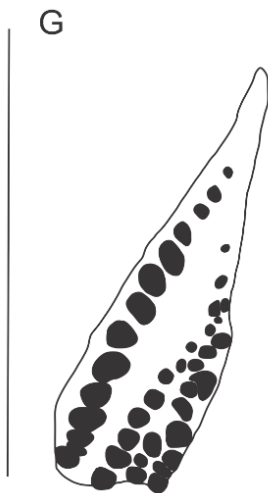
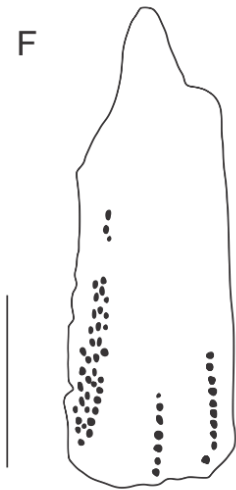
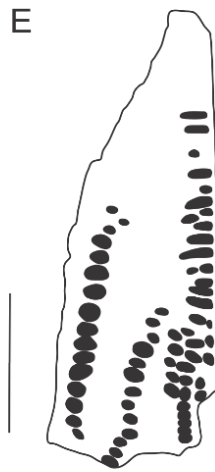
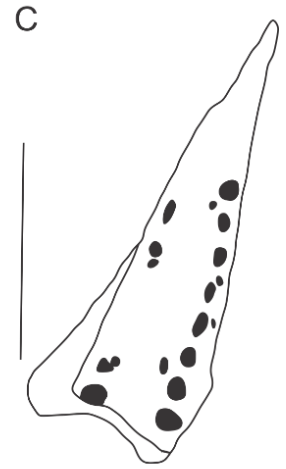
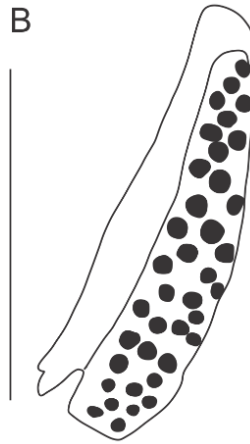
Source: Own author.

5. DISCUSSION

Rhynchosaurus articeps is of great historical importance, being the first taxon of Rhynchosauria to be described by the famous British anatomist and paleontologist Richard Owen in 1842.

In addition, it is also the first taxon in which the unique masticatory system is present (Figure 6, 7, 8 and 9 C). In opposition to non-Rhynchosauridae Rhynchosauria such as *Mesosuchus browni*, *Howesia browni* and *Eohyosaurus wolvaardti* which does not possess a groove and jaw apparatus (Dilkes, 1995, 1998, Butler et al., 2015) (Figure 9: A and B).

Figura 9 – Schematic drawings of the left maxillary dental plate: A: *Mesosuchus browni* (redrawn from Dilkes, 1998); B: *Howesia browni* (redrawn from Benton, 1905 and Dilkes, 1995); C: *Rhynchosaurus articeps*; D: *Ammorhynchus navajoi* (redrawn from Nesbitt 2004); E: *Brasinorhynchus mariantensis* (inverted and redrawn from Schultz, Langer & Montefeltro, 2016); F: *Stenaulorhynchus stockleyi* (redrawn from Benton, 1984); G: *Bentonyx sidensis* (redrawn from Sethapanichsakul et al, 2023); H: *Fodonyx spenceri* (redrawn from Langer, 2010); I: *Teyumbaita sulcognathus* (redrawn from Montefeltro et. al., 2010). Scale bars = 1 cm



Source: Own author.

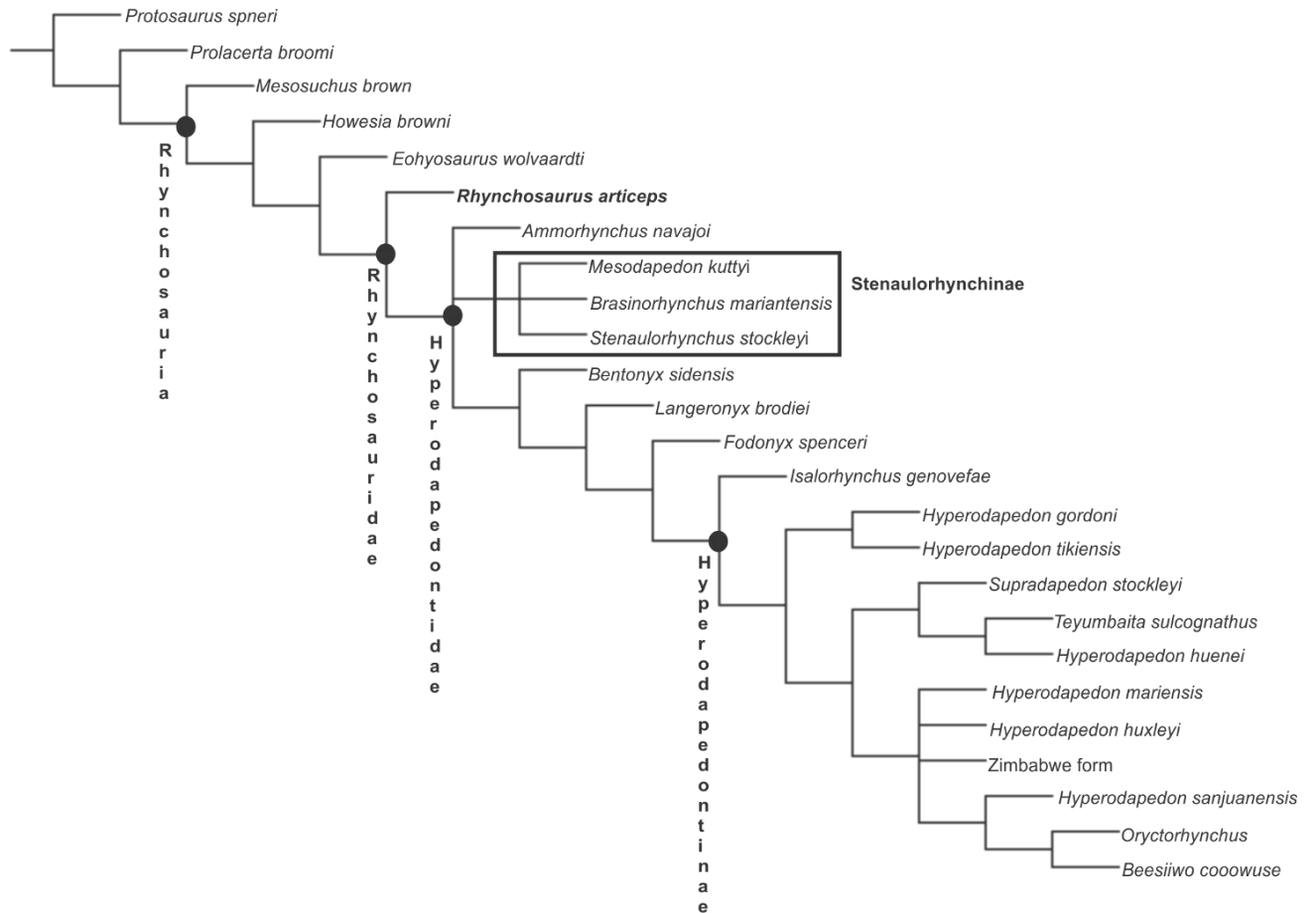
The updated parsimony analysis developed here resulted in six equally parsimonious trees with 235 steps (strict consensus is represented in Figure 10). Our strict consensus mostly agrees with the most recent analyses of Langer et al. (2017), Sues et al. (2020), and Fitch et al. (2023). In all these analyses the three South African forms from the Burgersdorp Group *Mesosuchus browni*, *Howesia browni*, and *Eohyosaurus wolvaardti* (Dilkes 1995, Butler et al., 2015, Ezcurra et al., 2016) form a paraphyletic array of taxa that are successively closer to the Rhynchosauridae (Figure 10). Also as in the three most recent analyses, *Rhynchosaurus articeps* is recovered as the basal most Rhynchosauridae and sister taxa of the Hyperodapedontidae clade (Figure 10). There is also a consensus among all more recent analyses on the presence of two main lineages of Hyperodapedontidae: the Stenaulorhynchinae (sensu Langer et al., 2010), and the other lineage composed by Hyperodapedontinae + all taxa closer to Hyperodapedontinae than to Stenaulorhynchinae (also called the non-Stenaulorhynchinae Hyperodapedontidae). Also, in accordance with the more recent analyses, our strict consensus recovered the clade Hyperodapedontinae (sensu Langer and Schultz, 2000) that is composed by all Late Triassic rhynchosaurs (*Isalorhynchus*, *Hyperodapedon* spp., *Teyumbaita*, *Oriktorhynchus*, *Beesiiwu*, and additional undescribed forms) and that encompasses the more diverse clade among rhynchosaurs (Ezcurra et al., 2021).

However, in more specific terms, as expected, our analysis is more congruent to the results from Langer et al. (2017), in which *Bentonyx* is recovered as closer to Hyperodapedontinae than Stenaulorhynchinae (contra Fetch et al, 2023), and which *Supradapedon*, *Teyumbaita* and *Hyperodapedon huenei* are recovered as basal hyperodapedontines, and not the most derived ones as recovered by Sues et al. (2020) and Fetch et al. (2023). Our results are also completely compatible with Langer's et al. (2017) regarding the relationships of hyperodapedontines. However, in our analysis, we recovered the clade composed by *Supradapedon* + *Teyumbaita* + *Hyperodapedon huenei* closer to the remaining hyperodapedontines than to the clade composed by *Hyperodapedon gordonii* + *Hyperodapedon tikiensis* (Figure 10).

The major difference between our analysis and Langer's et al. (2017) is the position of *Ammorhynchus navajoi*, which in some of the most parsimonious trees is referred to the Stenaulorhynchinae, as in Langer et al. (2017) and Fitch et al. (2023),

and in other most parsimonious trees it is closer to the Hyperodapedontinae (see consensus tree, Figure 10).

Figure 10 – Strict consensus of the 6 most parsimonious trees found in this analysis



Source: Own author.

5.1 Masticatory apparatus evolution in basal Rhynchosauria

Among the 129 characters proposed in our updated phylogeny of Rhynchosauria, about a third are related to the masticatory apparatus and teeth, so it is a region where morphological changes are more evident and expressive in the phylogeny (Langer et al., 2017; Langer et al., 2000b; Montefeltro, 2008; Montefeltro et al., 2013, Sues et al., 2020; Fitch et al.; 2023). In view of this, the focus of this study is to discuss the initial evolution of the unique masticatory apparatus in Rhynchosauridae, especially focused on the evolution of the basal taxa in this group. In the face of the updated scoring of the *Rhynchosaurus articeps* provided here, for the first time we were able to map the ancestral states for the origin of the unique groove and jaw apparatus of this clade.

The number of maxillary longitudinal sulcus is perhaps the most discussed trait in the dental evolution of rhynchosaurians, since the pre-cladistic period (Chatterjee, 1980; Benton, 1983b, 1984b, 1985). For a long time, it was proposed that all Mid-Triassic taxa possessed two longitudinal maxillary grooves, while the Late Triassic taxa possessed a single longitudinal maxillary groove (Langer, 1996). In this framework, the taxon *Rhynchosaurus* has been scored as possessing two longitudinal maxillary grooves (Chatterjee, 1980, Benton 1983, 1984, 1985, 1988, Dilkes 1995, 1998, Langer et al. 2000a). Posteriorly, with the description of *Teyumbaita sulcognathus* and *Hyperodapedon huenei*, which are Late Triassic taxa with two longitudinal maxillary sulci, these two taxa were assigned as possessing a transitional anatomy and all more derived hyperodapedontines had single grooved maxillae (Langer, 1996; Langer & Schultz, 2000; Langer et al., 2000a, Hone & Benton, 2008).

The first work to challenge this view was Nesbitt & Whatley (2004), with the description of the *Ammorhynchus navajoi*. However, perhaps the most important reinterpretation is derived from the change in the inclusivity of the Genus *Rhynchosaurus*. Benton (1990) described two new species assigned to this genus: “*R.*” *brodiei*, and “*R.*” *spenceri*. However, only specimens associated to the species “*R.*” *spenceri* had known specimens with assessable occlusal surface of the maxillae, and with the clear presence of two longitudinal maxillary sulci (Benton, 1990). As such, for the early phylogenetic analyses of Rhynchosauria, the operation taxonomic unity “*Rhynchosaurus*” was scored as having two longitudinal sulci (Benton, 1990, 1988,

Langer 1996, Langer & Schultz 2000ab, Langer et al., 2000ab). A series of posterior taxonomic works reinterpreted the genus *Rhynchosaurus*, and the only species associated to this genus remained *Rhynchosaurus articeps* (Hone and Benton, 2008, Langer et al., 2010, Ezcurra et al., 2016). Given that none of all known specimens of *R. articeps* possess assessable occlusal surface of the maxillae, the taxon has been rescored as “?” regarding the number of sulci in the maxillae presented by later authors (Montefeltro et al., 2010,2013, Langer et al., 2010, 2017, Butler et al., 2015).

With this new study it is possible, for the first time, to assess the anatomy of the occlusal surface of the maxillae of *Rhynchosaurus articeps* and show that this taxon possesses a single longitudinal sulcus on the occlusal surface of the maxillae (Figures 8 B and 6 A, B). With this new interpretation, it is possible to propose that the ancestral state for this character in Rhynchosauridae is the presence of a single longitudinal maxillary sulcus, and that there were at least two independent acquisitions of the second longitudinal sulcus, once in Stenaulorhynchinae, and once in Hyperodapedontinae, with a later reversion to the plesiomorphic state in Hyperodapedontinae.

Likewise, several other dentition characters at the origin of Rhynchosauridae were reinterpreted based on our 3D reconstruction of *Rhynchosaurus articeps*, such as teeth in the L1 row of the same size as other teeth; the presence of one medial longitudinal occlusal tooth row (M1); presence of crest-like lateral and medial maxillary tooth bearing areas; enlarged maxillary occlusal teeth, with each longitudinal row formed by reduced number of teeth; the presence of a single line of scattered lingual maxillary teeth; maxillary lingual teeth extending to the rostral half of maxillary length; maxillary lingual tooth crown medially oriented; the presence of a single dentary blade; lingual dentary teeth forming more than one row; presence of only conical dentary teeth; dentary teeth on the dentary lingual surface forming rows of well-spaced teeth; and dentary medial surface at caudal portion forming a bulged area projecting medially from the remaining area of the dentary (cushion-shaped).

6. CONCLUSIONS

The initial evolution of the unique masticatory apparatus in Rhynchosauridae, based on lectotype of *Rhynchosaurus articeps* (SHYMS 1), elucidated the ancestral state of the number of maxillary grooves in Rhynchosauridae as being the presence of a single maxillary groove, succeeded by at least two independent acquisitions of the medial groove, one in Stenaulorhynchinae and another in Hyperodapedontinae, with subsequent reversion to the plesiomorphic state, with a single maxillary sulcus, in Hyperodapedontinae.

REFERENCES

- BAIRD, D. Rhynchosaurs in the late triassic of nova scotia. **Geological Society of America Special Paper**, v. 73, p. 107, 1963. BENTON, M. The age of the rhynchosaur. **New Scientist**, v. 98, n. 1352, p. 9-13, 1983.
- BENTON, M. The Triassic reptile *Hyperodapedon* from Elgin: functional morphology and relationships. **Philosophical Transactions of the Royal Society of London. B, Biological Sciences**, v. 302, n. 1112, p. 605-718, 1983b
- BENTON, M. Tooth form, growth, and function in Triassic rhynchosaurs (Reptilia, Diapsida). **Palaeontology**, v. 27, n. 4, p. 737-776, 1984.
- BENTON, Michael J. The relationships and early evolution of the Diapsida. In: **Symposia of the Zoological Society of London**. 1984b. p. 575-596.
- BENTON, Michael J. Classification and phylogeny of the diapsid reptiles. **Zoological Journal of the Linnean Society**, v. 84, n. 2, p. 97-164, 1985.
- BENTON, M. J. The phylogeny of rhynchosaurs (Reptilia, Diapsida), and two new species. In: **Short Papers of the IV Symposium on Mesozoic Terrestrial Ecosystems**. 1988. p. 12-17. BENTON, Michael J. The species of *Rhyncosaurus*, a rhynchosaur (Reptilia, Diapsida) from the Middle Triassic of England. **Philosophical Transactions of the Royal Society of London. B, Biological Sciences**, v. 328, n. 1247, p. 213-306, 1990.
- BUTLER, Richard J. et al. A new species of basal rhynchosaur (Diapsida: Archosauromorpha) from the early Middle Triassic of South Africa, and the early evolution of Rhynchosauria. **Zoological Journal of the Linnean Society**, v. 174, n. 3, p. 571-588, 2015.
- CHATTERJEE, Sankar. A rhynchosaur from the Upper Triassic Maleri formation of India. **Philosophical Transactions of the Royal Society of London. B, Biological Sciences**, v. 267, n. 884, p. 209-261, 1974.
- CHATTERJEE, S. The evolution of rhynchosaurs. **Mémoires de la Société géologique de France, nouvelle série**, v. 139, n. 1658, p. 57-65, 1980.
- CUNNINGHAM, John A. et al. A virtual world of paleontology. **Trends in ecology & evolution**, v. 29, n. 6, p. 347-357, 2014.
- DILKES, David W. The rhynchosaur *Howesia browni* from the Lower Triassic of South Africa. **Palaeontology**, v. 38, n. 3, p. 665-686, 1995.
- DILKES, David W. The Early Triassic rhynchosaur *Mesosuchus browni* and the interrelationships of basal archosauromorph reptiles. **Philosophical Transactions of the Royal Society of London. Series B: Biological Sciences**, v. 353, n. 1368, p. 501-541, 1998.
- EZCURRA, Martín D. et al. The oldest rhynchosaur from Argentina: a Middle Triassic rhynchosaurid from the Chañares Formation (Ischigualasto–Villa Unión Basin, La Rioja Province). **Paläontologische Zeitschrift**, v. 88, n. 4, p. 453-460, 2014.

EZCURRA, Martín D.; MONTEFELTRO, Felipe; BUTLER, Richard J. The early evolution of rhynchosaurs. **Frontiers in Ecology and Evolution**, v. 3, p. 142, 2016.

EZCURRA, Martín D.; BUTLER, Richard J. The rise of the ruling reptiles and ecosystem recovery from the Permo-Triassic mass extinction. **Proceedings of the Royal Society B: Biological Sciences**, v. 285, n. 1880, p. 20180361, 2018.

EZCURRA, Martín D. et al. The stem-archosaur evolutionary radiation in South America. **Journal of South American Earth Sciences**, v. 105, p. 102935, 2021.

FITCH, Adam J. et al. A New Rhynchosaur Taxon from the Popo Agie Formation, WY: Implications for a Northern Pangean Early-Late Triassic (Carnian) Fauna. **Diversity**, v. 15, n. 4, p. 544, 2023. GOLOBOFF, Pablo A.; CATALANO, Santiago A. TNT version 1.5, including a full implementation of phylogenetic morphometrics. **Cladistics**, v. 32, n. 3, p. 221-238, 2016.

LANGER, M. C. Rincossauros sul-brasileiros: histórico e filogenia. **Unpublished Thesis, Instituto de Geociências, Universidade Federal do Rio Grande do Sul, Porto Alegre**, 1996.

LANGER, Max C.; FERIGOLO, Jorje; SCHULTZ, Cesar L. Heterochrony and tooth evolution in hyperodapedontine rhynchosaurs (Reptilia, Diapsida). **Lethaia**, v. 33, n. 2, p. 119-128, 2000a.

LANGER, Max C.; SCHULTZ, Cesar L. A new species of the Late Triassic rhynchosaur *Hyperodapedon* from the Santa Maria Formation of south Brazil. **Palaeontology**, v. 43, n. 4, p. 633-652, 2000b.

LANGER, Max C. et al. On *Fodonyx spenceri* and a new rhynchosaur from the Middle Triassic of Devon. **Journal of Vertebrate Paleontology**, v. 30, n. 6, p. 1884-1888, 2010.

LANGER, Max C.; DA ROSA, Átila AS; MONTEFELTRO, Felipe C. *Supradapedon* revisited: geological explorations in the Triassic of southern Tanzania. **PeerJ**, v. 5, p. e4038, 2017.

LAUTENSCHLAGER, Stephan. Reconstructing the past: methods and techniques for the digital restoration of fossils. **Royal Society Open Science**, v. 3, n. 10, p. 160342, 2016.

LAUTENSCHLAGER, Stephan. From bone to pixel—fossil restoration and reconstruction with digital techniques. **Geology Today**, v. 33, n. 4, p. 155-159, 2017.

LUCAS, SPENCER G.; HECKERT, ANDREW B.; HOTTON III, NICHOLAS. The rhynchosaur *Hyperodapedon* from the Upper Triassic of Wyoming and its global biochronological significance. Bulletin of the New Mexico Museum of **Natural History and Science**, v. 21, p. 149-156, 2002.

LORENSEN, William E.; CLINE, Harvey E. Marching cubes: A high resolution 3D surface construction algorithm. **ACM siggraph computer graphics**, v. 21, n. 4, p. 163-169, 1987.

FALK, Dean. Hominid brain evolution: The approach from paleoneurology. **American Journal of Physical Anthropology**, v. 23, n. S1, p. 93-107, 1980. GENTIL, Adriel R.; EZCURRA, Martín D. Reconstruction of the masticatory apparatus of the holotype of the rhynchosaur *Hyperodapedon sanjuanensis* from the Late Triassic of Argentina: implications for the diagnosis of the species. **Ameghiniana**, v. 55, n. 2, p. 137-149, 2017.

HONE, David WE; BENTON, Michael J. A new genus of rhynchosaur from the Middle Triassic of south-west England. **Palaeontology**, v. 51, n. 1, p. 95-115, 2008.

MONTEFELTRO, Felipe Chinaglia. Inter-relações filogenéticas dos rincossauros (Diapsida, Archosauromorpha). 2008. Dissertação (Mestrado em Biologia Comparada) - **Faculdade de Filosofia, Ciências e Letras de Ribeirão Preto, University of São Paulo**, Ribeirão Preto, 2008. doi:10.11606/D.59.2008.tde-24062008-161854.

MONTEFELTRO, Felipe Chinaglia; LANGER, Max Cardoso; SCHULTZ, Cesar Leandro. Cranial anatomy of a new genus of hyperodapedontine rhynchosaur (Diapsida, Archosauromorpha) from the Upper Triassic of southern Brazil. **Earth and Environmental Science Transactions of the Royal Society of Edinburgh**, v. 101, n. 1, p. 27-52, 2010.

MONTEFELTRO, Felipe Chinaglia et al. Postcranial anatomy of the hyperodapedontine rhynchosaur *Teyumbaita sulcognathus* (Azevedo and Schultz, 1987) from the Late Triassic of southern Brazil. **Journal of Vertebrate Paleontology**, v. 33, n. 1, p. 67-84, 2013. MUKHERJEE, Debarati; RAY, Sanghamitra. A new Hyperodapedon (Archosauromorpha, Rhynchosauria) from the Upper Triassic of India: implications for rhynchosaur phylogeny. **Palaeontology**, v. 57, n. 6, p. 1241-1276, 2014. NESBITT, Sterling J. et al. **The first discovery of a rhynchosaur from the upper Moenkopi Formation (Middle Triassic) of northern Arizona**. Museum of Paleontology, University of California, 2004. OWEN, Richard. Description of an extinct lacertian, *Rhynchosaurus articeps*, Owen, of which the bones and foot-prints characterize the upper New Red Sandstone at Grinshill, near Shrewsbury. **Trans. Camb. phil. Soc**, v. 7, n. 2, p. 355-369, 1842.

OWEN, Richard. Description of an Extinct Lacertian Reptile, *Rhynchosaurus articeps* Owen of which the Bones and Foot-prints characterize the Upper New Red Sandstone at Grinsill, near Shrewsbury. **Transactions of the Cambridge Philosophical Society**, v. 7, p. 355, 1848.

SALES, Marcos AF; SCHULTZ, Cesar L. Paleoneurology of *Teyumbaita sulcognathus* (Diapsida: Archosauromorpha) and the sense of smell in rhynchosaurs. **Palaeontologia Electronica**, v. 17, n. 1, p. 1-10, 2014.

SCARTEZINI, Caio A.; SOARES, Marina Bento. Assessing the diversity of hidden dental morphology in Hyperodapedontinae rhynchosaurs (Archosauromorpha, Rhynchosauria). **Historical Biology**, v. 35, n. 1, p. 58-73, 2023.

SCHULTZ, Cesar Leandro; LANGER, Max Cardoso; MONTEFELTRO, Felipe Chinaglia. A new rhynchosaur from south Brazil (Santa Maria Formation) and

rhynchosaur diversity patterns across the Middle-Late Triassic boundary. **PalZ**, v. 90, n. 3, p. 593-609, 2016.

SCHULTZ, Cesar Leandro; LANGER, Max Cardoso; MONTEFELTRO, Felipe Chinaglia. A new rhynchosaur from south Brazil (Santa Maria Formation) and rhynchosaur diversity patterns across the Middle-Late Triassic boundary. **PalZ**, v. 90, p. 593-609, 2016.

SETHAPANICHSAKUL, Thitiwoot; CORAM, Robert A.; BENTON, Michael J. New information on the cranial anatomy of the Middle Triassic rhynchosaurian reptile *Bentonyx sidensis*. **ACTA PALAEONTOLOGICA POLONICA** v.68, p. 53-62, 2023. SUES H-D, Olsen PE. Stratigraphic and temporal context and faunal diversity of Permian-Jurassic continental tetrapod assemblages from the Fundy rift basin, eastern Canada. *Atlantic Geology*, 2015. SUES, Hans-Dieter; FITCH, Adam J.; WHATLEY, Robin L. A new rhynchosaur (reptilia, Archosauromorpha) from the Upper Triassic of eastern North America. **Journal of Vertebrate Paleontology**, v. 40, n. 2, p. 177-568, 2020.

SUTTON, Mark D. Tomographic techniques for the study of exceptionally preserved fossils. **Proceedings of the Royal Society B: Biological Sciences**, v. 275, n. 1643, p. 1587-1593, 2008.

SUTTON, Mark; RAHMAN, Imran; GARWOOD, Russell. Virtual paleontology—An overview. **The Paleontological Society Papers**, v. 22, p. 1-20, 2016.

WHATLEY, Robin Leigh. Phylogenetic relationships of *Isalorhynchus genovefae*, the rhynchosaur (Reptilia, Archosauromorpha) from Madagascar. **University of California, Santa Barbara**, 2005.

ATTACHMENT A - Character list used in the parsimony analysis.

Characters 70 and 76 are treated as additive.

1. Skull dimensions: longer than broad (0); broader than long (1) (Benton, 1984).
2. Skull height: <50% of the midline length (0); >50% of the midline length (1) (Hone & Benton, 2008).
3. External nares: separate (0), single medial naris (1) (Benton, 1985).
4. Orbit orientation: mostly lateral (0); mostly dorsal (1) (Langer & Schultz, 2000).
5. Orbit with elevated rim along the jugal, postorbital, frontal, prefrontal and lacrimal: absent (0); present (1).
6. Orbital medial margin: rounded (0); forming a marked angle (1) (Montefeltro, Langer & Schultz, 2010).
7. Lower temporal fenestra: open ventrally (0), closed ventrally (1) (Dilkes, 1998).
8. Premaxilla ventral margin: horizontal (0), down-turned (1) (Benton, 1985).
9. Premaxilla and prefrontal contact: absent (0), present (1) (Dilkes, 1998).
10. Shape of rostral margin of nasal at midline: strongly convex with rostral process (0) or transverse with little convexity (1) (Dilkes, 1998).
11. Jugal and maxillary heights below the ventral border of the orbit: maxilla higher (0); jugal higher (1) (Benton, 1984).
12. Jugal-lacrimal contact: minimal (0); extensive contact of the jugal rostral process (1) (Whatley, 2005).
13. Anguli oris crest: absent (0); present (1) (modified from Benton, 1984).
14. Rostral extension of the anguli oris crest: restricted to the main body of the jugal (0); extending onto the rostral process of the jugal, but not the maxilla (1); extending onto the maxilla, but not the rostral process of the jugal (2) (modified from Benton, 1984).
15. Jugal surface dorsal to anguli oris crest: lacking a secondary crest (0); with a secondary anguli oris crest (1) (Langer & Schultz, 2000).
16. Lateral overlap of maxilla by jugal: absent or minimally expanded (0); well developed (1) (Whatley, 2005).
17. Jugal with multiple pits on the lateral surface of its main body: absent (0); present (1) (Butler et al. 2015).

18. Jugal subtemporal process: minimum height of the lower temporal bar >50% of the length of the process (0); minimum height of the lower temporal bar <50% of the length of the process (1)..
19. Jugal subtemporal process with a distinct lateroventral orientation with respect to the sagittal axis of the snout: absent (0); present (1) (Butler et al. 2015).
20. Relative widths of postorbital bar and lower temporal fenestra: <0.4 (0); >0.4 (1) (Langer & Schultz, 2000).
21. Dorsomedial surface of prefrontal near the orbital rim: flat or slightly concave (0); deeply concave (1) (Whatley, 2005).
22. Procumbent lacrimal and prefrontal rostralateral margin: absent (0); present (1) (Whatley, 2005).
23. Groove on the dorsal surface of the frontal: absent (0); present (1) (Dilkes, 1995).
24. Dorsal groove on frontal: longitudinally extended along most of the surface of the frontal (0); rostralaterally-to-caudomedially extended along the caudal half of the frontal (1) (Butler et al. 2015).
25. Well-marked 'V'-shaped crest along frontal-postfrontal contact, rostral to the margin of the supratemporal fossa: absent (0); present (1) (Montefeltro, Langer & Schultz, 2010).
26. Frontal and parietal midline lengths: frontal longer (0); parietal longer (1) (Benton, 1987).
27. Postfrontal: excluded from upper temporal fenestra border (0); forming the upper temporal fenestra border (1) (Dilkes, 1998).
28. Postfrontal dorsal surface: flat (0); markedly concave (1) (Dilkes, 1995).
29. Caudal extension of the caudal process of the postorbital: considerably rostral to the level of the caudal border of the infratemporal fenestra (0); at level with the caudal border of the infratemporal fenestra (1) (modified from Dilkes, 1998).
30. Postorbital rostroventral process: expanding ventral to the level of the orbital midpoint (0); expanding dorsally to orbital height midpoint (1) (Dilkes, 1998).
31. Postorbital ventral process: expands rostral to the jugal (0); fits dorsal to the jugal (1) (Whatley, 2005).
32. Postorbital-parietal suture: visible in dorsal view (0); hidden in dorsal view (1) (Dilkes, 1998).
33. Parietals: separate (0), fused (1) (Benton, 1985).

34. Parietal foramen: always, or sometimes, present (0), always absent (1) (Benton, 1985).
35. Parietal table: broad (0), constricted and with sagittal crest (1) (Dilkes, 1998).
36. Parietal body: not expanded laterally at midlength (0); expanded laterally at midlength (1) (Montefeltro, Langer & Schultz, 2010).
37. Parietal transverse process: caudolaterally directed (0); laterally directed (1) (Montefeltro, Langer & Schultz, 2010).
38. Distal tip of parietal transverse process: not rostroventrally curved (0); rostroventrally curved (1) (modified from Montefeltro, Langer & Schultz, 2010).
39. Squamosal ventral process: thinner than 50% of dorsoventral length (0); broader than over 50% of dorsoventral length (1) (Benton, 1990).
40. Squamosal medial process: short, forming less than half of the caudal border of the supratemporal fenestra (0); long, forming entire or almost entire caudal border of the supratemporal fenestra (1) (Butler et al. 2015).
41. Relative position of quadratojugal and squamosal processes: squamosal ventral process rostral to quadratojugal dorsal process (0); squamosal ventral process overlapping the quadratojugal dorsal process (1) (Whatley, 2005).
42. Quadratojugal rostral process: completely absent (0), present (1) (Dilkes, 1998).
43. Supratemporal: present (0); absent (1) (Benton, 1984).
44. Supratemporal with a bifurcated medial border, in which a ventromedial process extends underneath the caudolateral process of the parietal: present (0); absent (1) (Butler et al. 2015).
45. Pterygoid midline suture length: greater than or equal to the distance between the caudal margin of the suture and the basipterygoid articulation (0); less than the distance between the caudal margin of the suture and the basipterygoid articulation (1) (Whatley, 2005).
46. Ectopterygoid reaches lateral corner of transverse flange of pterygoid: no (0), yes (1). (Dilkes, 1998)
47. Elements forming the border of the suborbital fenestra: pterygoid, ectopterygoid, palatine, and maxilla (0); pterygoid, ectopterygoid and palatine only (1) (Dilkes, 1995).
48. Supraoccipital shape: plate-like (0); inverted V-shape (1). (Dilkes, 1995)
49. Occipital condyle position: rostral to craniomandibular articulation (0); aligned to craniomandibular articulation (1) (Benton, 1984).

50. Basioccipital and basisphenoid/parasphenoid lengths: basisphenoid/parasphenoid longer (0); basioccipital longer (1) (Langer & Schultz, 2000).
51. Relative positions of the basipterygoid process of the basisphenoid and the ectopterygoid process of the pterygoid: basipterygoid process of the basisphenoid caudal to ectopterygoid process of the pterygoid (0), or at the same level (1) (Dilkes, 1995).
52. Basipterygoid process dimensions (dorsoventral length, rostrocaudal width): longer than wide (0); wider than long (1) (Langer & Schultz, 2000).
53. Jaw symphysis: formed largely by dentary (0), formed only by splenial (1) (Dilkes, 1998).
54. Divergence of dentaries in front of symphysis: absent (0), present (1) (Dilkes, 1998).
55. Mandible depth: <0.25 of the total length (0); >0.25 of the total length (1) (Benton, 1984).
56. Dentary length: half, or less, than the total mandibular length (0); greater than half of the total mandibular length (1) (Benton, 1990).
57. Premaxillary teeth: present (0), absent (1) (Benton, 1985).
58. Tooth implantation: subthecodont or thecodont (0), ankylothecodont (1) (Benton, 1985).
59. Maxilla occlusal ventral margin: horizontal (0), convex (1). (modified from Dilkes, 1998).
60. Tooth occlusion: single sided overlap (0), flat occlusion (1), blade and groove jaw apparatus, where dentary blade(s) fit precisely into maxillary groove(s) (2) (Benton, 1985).
61. Vomerine teeth: present (0), absent (1) (Dilkes, 1998).
62. Palatine teeth: present (0), absent (1) (Dilkes, 1998).
63. Pterygoid teeth: present (0), absent (1). (Modified from Benton, 1983a and Ezcurra et al. 2015).
64. Pterygoid teeth: present as two or more rows of bottom-like teeth (0); present, but single distinct row of teeth (1) (Benton, 1983a, 1983a and Ezcurra et al. 2015).
65. Medial maxillary groove: absent (0); present (1) (Benton, 1984).
66. Medial maxillary groove: not reaching the rostral half of the maxilla (0), reaching the rostral half of the maxilla (1) (Benton, 1984).

67. Maxillary area lateral to main groove: narrower than the medial area (0); same width or broader than the medial area (1) (Benton, 1990).
68. Maxillary cross-section lateral to main groove: (0); cushion-shaped (1) (Langer, Ferigolo & Schultz, 2000).
69. Tooth rows lateral to main maxillary groove: a single clear row (0); more than one clear row (1) (Langer & Schultz, 2000).
70. Number of tooth rows medial to main maxillary groove (at the caudal half of the maxilla): single row (0), two rows (1); three or more tooth rows (2) (Langer, Ferigolo & Schultz, 2000, modified from Schultz et al. 2016).
71. Occlusal tooth rows on the rostral half of the maxilla: four or more tooth rows (0); fewer than four tooth rows (1) (Whatley, 2005).
72. Maxillary lingual teeth: absent (0); present (1) (Benton, 1984).
73. Maxillary lingual teeth: scattered teeth (0); large number of teeth on the medial surface of the bone (1) (Benton, 1984).
74. Maxillary teeth: only conicals (0); conicals and 'pyramidal' (1) (Whatley, 2005).
75. Dentary teeth: only conical (0); conical and rostrocaudally compressed (1) (Whatley, 2005).
76. Number of rows of teeth on dentary: one (0), two (1), more than two full rows (2). (Benton, 1983a).
77. Caudal-most dentary teeth: on the rostral half of lower jaw (0); on the caudal half of lower jaw (1) (Langer & Schultz, 2000).
78. Lingual dentary teeth: absent (0); present (1) (Benton, 1984).
79. Lingual dentary teeth: forming one row (0); forming more than one row (1) (Benton, 1984).
80. Dentary teeth on the dentary lingual surface: forming rows of well-spaced teeth (0); crowded (1) (Benton, 1985, rewritten from Schultz et al. 2016).
81. Axis ventral keel: present (0); absent (1) (Montefeltro et al., 2013).
82. Axial parapophysis: present (0); absent (1) (Montefeltro et al., 2013).
83. Cervical postaxial vertebrae ventral keel: absent (0); present (1) (Montefeltro et al., 2013).
84. Truncal vertebrae with ossified intercentrum: present (0); absent (1) (Evans, 1988).
85. Epiphyses on third cervical vertebra: spine-shaped (0); crest-shaped (1). This character was firstly modified from Whatley (2005), and we decide to restrict the character to the third cervical vertebrae.

86. Position of the transverse process of cranial truncal vertebrae: at the level of prezygapophysis (0); caudally located in the vertebra centrum (1) (Montefeltro et al., 2013).
87. Second sacral vertebra: with a notch between the iliac articular surface and the caudal process (0); caudal process continuous to the iliac articular surface (1) (Dilkes, 1998).
88. Caudal vertebrae, neural spine height versus proximodistal length at its base in proximal caudal vertebrae: <2.20 (0); ≥ 2.20 (1) (Dilkes, 1998).
89. Interclavicle: caudal process longer than twice the lateral processes (0); caudal process shorter than twice the lateral process (1) (Dilkes, 1998).
90. Supinator process on the external surface of humeral ectepicondyle: hook-shaped (0); formed by a low supinator ridge and ligament groove (1) (Montefeltro et al., 2013).
91. Caudal process of the coracoid: present (0); absent (1) (Benton, 1984).
92. Dorsal margin of the ilium: cranial process $<15\%$ of the length of the caudal process (0); cranial process $>15\%$ of the length of the caudal process (1) (Dilkes, 1995).
93. Pubic tubercle on the lateral surface of the pubic shaft: present (0); absent (1) (Whatley, 2005).
94. Internal trochanter: continuous with the femoral head (0); separated from femoral head (1) (Whatley, 2005).
95. Crest on craniomedial region of tibial shaft: absent (0); present (1) (Montefeltro et al., 2013).
96. Relative size of astragalar articular facets: tibial facet greater than centrale facet (0); centrale facet greater than tibial facet (1) (Langer & Schultz, 2000).
97. Metatarsal I: longer than broad (0); broader than long (1) (Hone & Benton, 2008).
98. Sacral vertebrae and ribs, shape of the caudal projection of the bifurcated distal end of the second sacral rib: tapering (0); squared (1) (Dilkes 1998).
99. Caudal vertebrae, median longitudinal groove on the ventral surface of the centrum of the first two caudals: absent (0); present (1) (Dilkes, 1998).
100. Metatarsus, length of metatarsal I versus metatarsal III: <0.45 (0); ≥ 0.45 (1) (Dilkes 1998).
101. Caudal orbital margin and caudal margin of maxillary tooth bearing area: at the same level (0), caudal orbital margin located caudally (1) (Schultz et al. 2016).

102. Dorsal nasal profile in lateral view: nasal inclined rostrally (0); nasal horizontal oriented, rostral edge in level with caudal edge (1) (Schultz et al. 2016).
103. Participation of the frontal in orbital margin: frontal forming great part of the median section of orbital dorsal border (0), prefrontal and postfrontal closer to, or contacting each other reducing the participation of the frontal in dorsal orbital border (1) (Schultz et al. 2016).
104. Squamosal body: restricted, forming a restricted intertemporal bar (0), developed and forming a plate-like intertemporal bar (1) (Schultz et al. 2016).
105. Rounded depression on the ventral surface of basisphenoid: absent (0), present (1) (Schultz et al. 2016).
106. Dentary medial surface at caudal portion: flat (0), forming a bulged area projecting medially from the remaining area of the dentary (1) (Schultz et al. 2016).
107. Curvature of the maxillary caudal border in lateral view: caudal border of maxillae curves gentle towards the jugal (0), caudal border of maxillae curves strongly towards the jugal so that the caudal teeth face caudoventrally (1) (Schultz et al. 2016).
108. Extension of the lateral, or only, maxillary groove: along the whole occlusal surface of maxilla (0); limited to the caudal half of maxillary occlusal surface (1) (Schultz et al. 2016).
109. Maxillary cross-section medial to main groove: crest-shaped (0); cushion-shaped (1) (Schultz et al. 2016).
110. Size of maxillary occlusal teeth: enlarged teeth with each longitudinal row formed by reduced number of teeth (0), reduced teeth with each longitudinal row formed by great number of teeth (1) (Schultz et al. 2016).
111. Maxillary lingual teeth: restricted to caudal half of the maxilla (0), extending to the rostral half of maxillary length (1) (Schultz et al. 2016).
112. Maxillary lingual tooth crown orientation: medially oriented, perpendicular to maxillary medial wall (0), ventrally directed parallel to maxillary medial wall (1) (Schultz et al. 2016).
113. Jugal height/length ratio: < 0.5 (0), >0.5 (1) (Modified from Mukherjee & Ray 2014).
114. Frontal pair: Longer than broad (0), Broader than long (1) (Benton 1983, Mukherjee & Ray 2014).

115. Proportion of maxillary tooth plate: Width at caudal end/Length < 0.3 (0), >0.3 (1) (Modified from Mukherjee & Ray 2014).
116. Three bulbous processes or convexities on the cranial surface of the axial centrum: absent (0), present (1) (Mukherjee & Ray 2014).
117. Coracoid foramen: restricted to coracoid (0), shared between scapula and coracoid (1) (Modified from Langer & Schultz 2000, Mukherjee & Ray 2014: 58).
118. Ratio between humeral (HL) and femoral (FL) lengths: HL/FL < 1 (0), HL/FL ≥ 1 (1) (Mukherjee & Ray 2014).
119. Presence of a hook-shaped process at the maxilla-premaxilla suture above the dentigerous area: absent (0), present (1) (new character).
120. Paraoccipital process of opisthotic: curved ventrally (0), straight (1) (Langer et al. 2017).
121. Number of tooth rows lateral to the main groove: lesser than the number of medial tooth row (0), as many as or greater than the number of medial tooth rows (1) (Langer et al. 2017).
122. Size of teeth in rows L1 and L2: same size as other teeth (0), teeth in L1 or L2 larger than other teeth (1) (Langer et al. 2017).
123. Medial most row of occlusal tooth at caudal region of maxilla: strictly occlusal (0), medially displaced and crowns with not strictly occlusal direction (1) (Langer et al. 2017).
124. Maxilla, posterior half of the lateral tooth bearing area: entire transverse surface covered with teeth (0); presence of an edentulous lateral platform (1) (new character).
125. Jugal, anterolateral surface of the posterior process: mostly flat (0); with a posterodorsally well rimmed depression that merges gradually anteriorly with the main body of the bone (1) (new character).
126. Quadratojugal, shape of the main body: subtriangular, with a broad dorsal ramus (0); crescent-shaped, with a strongly anteriorly curved and anteroposteriorly narrow dorsal ramus (1). *Isalorhynchus genovefae* possesses an overall anteriorly curved main body, but it has a posterior process that results in a different morphology to that of *Hyperodapedon huxleyi* and *Hyperodapedon huenei*. As a result, the Malagasy species was scored as (0) (new character).
127. Parabasisphenoid, position and orientation of the entrance of the internal carotid arteries: on the ventral surface and immediately posteromedial to the bases of

the basipterygoid processes, facing mainly ventrally (0); on the ventral surface and between the bases of the basipterygoid processes close to the level of their mid-length, facing mainly anteriorly (1) (new character).

128. Parabasisphenoid, distal end of the basipterygoid processes in ventral view: well-separated from each other, clearly exposing the ventral surface of the parabasisphenoid between them (0); almost touching each other in the median line and restricting the interbasipterygoid process space to a narrow furrow, also resulting in basal articulation of the pterygoids approaching very close to each other (1) (new character).
129. Scapula, lateral development of the acromion process: low and not more developed than the transverse thickness of the scapular neck (0); hypertrophied as a shelf-like structure more developed than the thickness of the scapular neck (1) (new character).

ATTACHMENT B - SYNAPOMORPHY LIST

Synapomorphies common to 6 trees
(Node numbers refer to nodes in consensus)

Protorosaurus_speneri:

All trees:

No autapomorphies:

Prolacerta_broomi:

All trees:

No autapomorphies:

Mesosuchus_browni:

All trees:

Char. 44: 1 --> 0

Char. 82: 1 --> 0

Char. 98: 0 --> 1

Howesia_browni:

All trees:

No autapomorphies:

Eohyosaurus_wolvaardti:

All trees:

No autapomorphies:

Rhynchosaurus_articeps:

All trees:

Char. 27: 1 --> 0

Char. 78: 1 --> 0

Langeronyx_brodiei:

All trees:

Char. 22: 1 --> 0

Char. 78: 1 --> 0

Char. 112: 1 --> 0

Char. 121: 0 --> 1

Stenaulorhynchus_stockleyi:

All trees:

Char. 5: 0 --> 1

Char. 69: 1 --> 0

Char. 113: 0 --> 1

Char. 125: 0 --> 1

Brasinorhynchus mariantensis:

All trees:

Char. 1: 0 --> 1

Char. 4: 1 --> 0

Char. 35: 1 --> 0

Char. 69: 1 --> 2

Char. 81: 0 --> 1

Bentonyx sidensis:

All trees:

Char. 5: 0 --> 1

Char. 50: 0 --> 1

Char. 64: 0 --> 1

Char. 67: 0 --> 1

Char. 69: 1 --> 2

Fodonyx spenceri:

All trees:

Char. 64: 0 --> 1

Char. 105: 0 --> 1

Isalorhynchus genovefae:

All trees:

Char. 14: 0 --> 1

Char. 20: 1 --> 0

Char. 75: 2 --> 1

Char. 78: 1 --> 0

Char. 88: 0 --> 1

Char. 121: 0 --> 1

Char. 123: 0 --> 1

Hyperodapedon huenei:

All trees:

Char. 119: 0 --> 1

Char. 125: 0 --> 1

Zimbabwe form:

All trees:

Char. 71: 0 --> 1

Beesiiwo coowuse:

All trees:

No autapomorphies:

Hyperodapedon tikiensis:

All trees:

Char. 120: 0 --> 1

Char. 128: 0 --> 1

Hyperodapedon_huxleyi:

All trees:
 Char. 121: 0 --> 1
 Some trees:
 Char. 86: 0 --> 1
 Char. 88: 0 --> 1
 Char. 117: 0 --> 1
 Char. 128: 0 --> 1

Hyperodapedon_gordoni:

All trees:
 Char. 66: 1 --> 0
 Char. 80: 0 --> 1
 Char. 122: 0 --> 1

Hyperodapedon_mariensis:

All trees:
 No autapomorphies:

Hyperodapedon_sanjuanensis:

All trees:
 No autapomorphies:

Supradapedon:

All trees:
 No autapomorphies:

Ammorhynchus:

All trees:
 No autapomorphies:

Mesodapedon:

All trees:
 Char. 68: 0 --> 1

Teyumbaita_sulcognathus:

All trees:
 Char. 5: 0 --> 1
 Char. 17: 1 --> 0
 Char. 27: 0 --> 1
 Char. 67: 1 --> 0
 Char. 79: 0 --> 1
 Char. 123: 0 --> 1
 Char. 127: 0 --> 1

Oryctorhynchus:

All trees:
 No autapomorphies:

Node 30:

All trees:
No synapomorphies

Node 31:

All trees:
Char. 2: 0 --> 1
Char. 8: 0 --> 1
Char. 22: 0 --> 1
Char. 27: 0 --> 1
Char. 59: 0 --> 1
Char. 75: 0 --> 2
Char. 92: 1 --> 0
Char. 99: 1 --> 0
Char. 109: 1 --> 0

Node 32:

All trees:
Char. 9: 0 --> 1
Char. 33: 0 --> 1
Char. 58: 0 --> 1
Char. 71: 0 --> 1

Node 33:

All trees:
Char. 28: 0 --> 1

Node 34:

All trees:
Char. 4: 0 --> 1
Char. 16: 1 --> 0
Char. 18: 0 --> 1
Char. 35: 0 --> 1
Char. 39: 0 --> 1
Char. 47: 0 --> 1
Char. 59: 1 --> 2
Char. 60: 0 --> 1
Some trees:
Char. 72: 0 --> 1

Node 35:

All trees:
Char. 11: 0 --> 1
Char. 27: 1 --> 0
Char. 100: 1 --> 0
Char. 110: 1 --> 0

Node 36:

Some trees:
Char. 13: 2 --> 0

Char. 62: 0 --> 1
Char. 72: 1 --> 0

Node 37:

All trees:
Char. 10: 0 --> 1
Char. 20: 0 --> 1
Char. 49: 0 --> 1
Char. 79: 0 --> 1
Char. 96: 0 --> 1
Char. 103: 0 --> 1
Char. 106: 0 --> 1
Char. 122: 1 --> 0

Node 38:

All trees:
Char. 64: 0 --> 1

Node 39:

All trees:
Char. 79: 1 --> 0
Char. 108: 0 --> 1

Node 40:

All trees:
Char. 3: 0 --> 1
Char. 4: 1 --> 0
Char. 6: 0 --> 1
Char. 13: 0 --> 1
Char. 15: 0 --> 1
Char. 38: 0 --> 1
Char. 40: 0 --> 1 Char. 54: 0 --> 1
Char. 66: 0 --> 1
Char. 67: 0 --> 1
Char. 71: 1 --> 0
Char. 73: 0 --> 1
Char. 74: 0 --> 1
Char. 76: 0 --> 1

Node 41:

All trees:
Char. 64: 0 --> 1
Char. 66: 1 --> 0

Node 42:

All trees:
Char. 71: 0 --> 1
Char. 122: 0 --> 1

Node 43:

All trees:

Char. 26: 0 --> 1

Node 44:

All trees:

Char. 29: 0 --> 1

Char. 30: 0 --> 1

Char. 51: 0 --> 1

Char. 68: 0 --> 1

Char. 70: 1 --> 0

Char. 84: 0 --> 1

Node 45:

All trees:

Char. 75: 2 --> 1

Char. 120: 0 --> 1

Some trees:

Char. 78: 1 --> 0

Node 46:

All trees:

Char. 70: 0 --> 1

Char. 114: 1 --> 0

Node 47:

All trees:

Char. 75: 1 --> 0

Char. 77: 1 --> 0

Char. 108: 1 --> 0

Node 48:

All trees:

Char. 81: 0 --> 1

Char. 115: 0 --> 1

ATTACHMENT C - OTUs USED IN THE PHYLOGENETIC ANALYSIS

Ingroup and outgroup operational taxonomic units used in the phylogenetic analysis. Sources of data for scoring are listed for each taxon

Ammorhynchus navajoi: Nesbitt & Whatley (2004).

Bentonyx sidensis: Sethapanichsakul et. al. (2023)

Eohyosaurus wolvaardti: Butler et al. (2015).

Fodonyx spenceri: Benton (1990).

Brasinorhynchus mariantensis: Schultz et al. (2016)

Howesia browni: Dilkes (1995).

Hyperodapedon gordonii: Benton (1983).

Hyperodapedon huenei: Langer & Schultz (2000).

Hyperodapedon huxleyi: Chatterjee (1974).

Hyperodapedon mariensis: Langer et. al. (2017)

Hyperodapedon sanjuanensis: Langer et. al. (2000b)

Hyperodapedon tickensis: Mukherjee & Rey (2014).

Hyperodapedon sp. Nova Scotia: Baird (1963), Sues & Olsen (2015), Sues et. al. (2020)

Hyperodapedon sp. Zimbabwe: Raath et al. (1992).

Hyperodapedon sp. Wyoming Beesiiwo coowuse: Lucas et al. (2002). Fitch et. al. (2023)

Isalorhynchus genovefae: Buffetaut (1983); Whatley (2005).

Langeronyx brodiei: Chatterjee (1980).

Mesosuchus browni: Dilkes (1998).

Prolacerta broomi: Modesto & Sues (2004).

Protorosaurus speneri: Gottman-Quesada & P. M. Sander (2009).

Rhynchosaurus articeps: SHYMS 1

Stenaulorhynchus stockleyi: Huene (1938).

Teyumbaita sulcognathus: Montefeltro et al. (2010).

ATTACHMENT D - TAXON-CHARACTER MATRIX

Taxon-character matrix used in the phylogenetic analysis. Missing data are marked as '?', nonapplicable characters as '-'

Protorosaurus_speneri

000000?000000--00?00000-00000000(0 1)?10001???1????0?????0010000??00----
 ---0-00010--????1-010010?10000 ?11?00??---1--00-?0000----????0

Prolacerta_broomi

0000000100000—011000000000000000000000000111000000000101000000-----
 0-00000--0010-00001001000010110000?---1--00-00000----0-0?0

Mesosuchus_browni

00100001100000110000100001000010000000000000000000000000000010000 -----0-
 00200--00000001010000000110100000---0--00-0?001----0-0?0

Howesia_browni

00?0000??10?????1100001000010?00111000?0??0?10000000?????111?000-----
 0100020??0?0?001??00000010??0?0?0--01??00????????10??0??

Eohyosaurus_wolvaardti

00?00?0??0?12001100?????0?100?1?1000000100??0??0??00?1110?00-----
 ?10002?110????????????????????1??0?00--0?01??????0????00???

Rhynchosaurus_articeps

00101001110012000110001101001000111100010101110100001101111211000-
 00001110020110??0??00(0 1)0?0??01000001000?1000010100?00010-1000000

Langeronyx_brodiei

??1010?11?1110000?1?100?0??0?00????????????????0????011??1112?????0?0
 00(0 1)110002?101????????????????????000??0100001000?????0100?????

Stenaulorhynchus_stockleyi

0010110111101200?110100?1101100011110101010111110100110011121101110
000111002011110000000001001010?01111111101101100000000001000

Brasinorhynchus_mariantensis

01100001111012000110100?110110011110110?010???01010011??11121101110
002111002?111110????????????????????10111111011?1000??0100?000?0?

Bentonyx_sidensis

001011?1111010000?10101101011?01111110?1?1011?11011011??1112111?110
102?10002?111????????????????????110110100011?0????010?00??0??

Fodonyx_spenceri

11?01?0???1?1000?11????????????????????????????????11?????11011112111?100
0011100020110????????????????????????????????1?110100????????????000000???

Isalorhynchus_genovefae

11110?1111111111011101?????0100?111?1?1?11??0?1?110011111112111?0?1
10(1 2)10-1111100??11000011110111?1?00??001010??1?1?00?0101?000?

Hyperodapedon_huenei

11110011111111110111110?0110111111111011111?0111110111111112111?100
1120101121110????????????????????????010101101000101???11001011?0?

Zimbabwe form

?1????1??1?1??1????????????????????????????????1??????1??1112?11?0?1
11(1 2)010111?100????????????????????????????01010????1???0?1000?????

Beesiiwo_cooowuse

??????1??11?2????0?1
?1?10-110?0--????????????????????????????0?0????0?????1?0?????

Hyperodapedon_tikiensis

??11??11?1?110?0????????????????????????????????11?11??112?11?0?1
11200-112?1100111?0??1?1?111?????????0(0 1)1010--??11????1000??001

Hyperodapedon_huxleyi

11110011111111010011?110011011111111011111?111111011111112111?0?1
11200-111110000?110101111?1111??00101001010--1010110011001(0 1)101

Hyperodapedon_gordoni

11110011111111010111?110010011101111011111?111111011111112111?0?0
11(12)00011(12)11(01)0111110?0011111111??00101001010—
10111100001000100

Hyperodapedon_mariensis

111100111111110100111110011011111111011111?(01)(01)1111011111112111
?0?111200-1111100??1?00?011??1?1?1??0101001010--101?100010(01)010(0
1)00

Hyperodapedon_sanjuanensis

111100111111110101111110011011111111011111?011111011111112111?0?1
11200-11010--?011?00?0111?111?1??0101001000--1010??001000(0 1)0(0 1)0?

Supradapedon

????????????11?1??112????0?1
1120101????????????????????????1????????????????101000??1?????0010?????

Ammorhynchus

??1112????0?0
0011110??11????????????????????????????????100111??0?????00???????

Mesodapedon

??1???1?2????110
011111002?111????????????????????????????????011??0?????00???????

ATTACHMENT E - Most Parsimonious trees

